THESIS FOR THE DEGREE OF LICENTIATE OF ENGINEERING

Sorption of Cs, Ba, Co, and Eu onto biotite: experiments and modelling

Pawan Kumar

Nuclear Chemistry
Department of Chemistry and Chemical Engineering
CHALMERS UNIVERSITY OF TECHNOLOGY
Gothenburg, Sweden 2023

Sorption of Cs, Ba, Co, and Eu onto biotite: experiments and modelling

PAWAN KUMAR

Technical report no 2023:15

Department of Chemistry and Chemical Engineering
Chalmers University of Technology
SE-412 96 Gothenburg
Sweden
Telephone + 46 (0)31-772 1000

Cover:
Batch sorption experiment with biotite at three different ionic strengths (0.001M, 0.01M and 0.1M) at five different pH (5-9) and at 25ºC.

Printed by:
Chalmers Digitaltryck
Gothenburg, Sweden 20

Sorption of Cs, Ba, Co, and Eu onto biotite: experiments and modelling

Pawan Kumar
Nuclear Chemistry
Department of Chemistry and Chemical Engineering
CHALMERS UNIVERSITY OF TECHNOLOGY
Gothenburg, Sweden 2023

Abstract

The sorption of ^{134}Cs, ^{133}Ba, ^{60}Co and ^{152}Eu, all at about [~10^{-8} M] onto biotite mineral was studied using the batch method with S: L = 1:50 at three different ionic strengths (0.001, 0.01 and 0.1M $NaClO_4$) and five different pH (5,6,7,8,9) at 25°C for up to two months in an inert atmosphere glovebox. The results revealed that the sorption of all metals was dependent on both pH and ionic strength.

At 25°C, the measured sorption distribution coefficients (R_d -values) for 0.001 M were (pH 5-9): (Cs) 0.6-1.2, (Ba) 0.3-8.3, (Co) 0.01-1.9 and (Eu) 2.7-18 m^3/kg, respectively. For I = 0.01 M, the corresponding results were (Cs) 0.1-0.7, (Ba) 0.01-4.4, (Co) 0.01-7.5 and (Eu) 0.2-4.3 m^3/kg, respectively. For I= 0.1M, the corresponding results were (Cs) 0.01-0.2, (Ba) 0.03-0.4, (Co) 0.01-4.7 and (Eu) 2.1-6.7 m^3/kg.

The surface acidity constants for the amphoteric surface site of biotite mineral were determined with the continuous potentiometric titration on a biotite suspension to $pKa_1 = 4.77 \pm 0.30$ and $pKa_2 = -6.82 \pm 0.20$. These acidity constants were obtained by fitting titration data through the use of PHREEQC and PYTHON code optimization routines.

The biotite size fraction of 0.25-0.5 mm was characterized for acidic site density (ASD), cation exchange capacity (CEC) and the specific surface area (SSA) and were determined to be 6.7μmol/m^2, 1.01± 0.03 meq/100g and 0.47 m^2/g by using tritium uptake, ammonium acetate (NH_4Ac), and Kr-BET adsorption methods, respectively.

To model the experimental sorption data, PHREEQC geochemical modelling software coupled with PYTHON code optimization routines was used. The results shows that a two-step protolysis (2-pKa) non-electrostatic model (NEM) representing edge site with one additional ion-exchange site representing basal plane site is sufficient to reproduce the data for all four metals.

Key words: Surface Complexation, titration, Cs, Eu, Co, Ba, Biotite, Sorption

List of Publications and Manuscripts

This thesis is based on the following publication and manuscript.

Paper 1
S. Holgersson and P. Kumar, "A literature review on thermodynamic sorption models of radionuclides with some selected granitic mineral." Frontiers in Nuclear Engineering, 2, 2023.

Paper 2
P, Kumar, S. Holgersson, and C. Ekberg, "Cs, Ba, Co, and Eu sorption on biotite at pH 5-9 and varying ionic strength." (Will be submitted to Radiochimica Acta)

Abbreviations

ASD - Acidic Site Density

BET - Brunauer -Emmett-Teller

CA - Component Additive

CCM - Constant Capacitance Model

CD-Music - Charge-Distribution Multi-Site Surface Complexation Model

CEC - Cation Exchange Capacity

DLM - Diffuse Layer Model

DFT - Density Functional Theory

HTO - Tritium Water

NEM - Non-electrostatic Model

SCM - Surface Complexation Model

SSA - Specific Surface Area

TLM - Triple Layer Model

TSM - Thermodynamic Sorption Model

Contents

1. Introduction

The generation of energy by burning fossil fuels has a negative impact on both global and local environment and human health, due to the release of carbon dioxide and soot particles to the air. Fortunately, there are alternative technologies such as hydro, solar, and wind energy that can produce electricity with less harmful effects. However, these sources alone are not sufficient to replace fossil fuels completely, which accounted for no less than 84% of global energy production in 2019 (OurWorldinData.org).

It is clear that a serious attempt to reduce emissions also must include nuclear power in energy production. After more than 70 years of using hundreds of nuclear power plants (NPPs) worldwide, it can be said that nuclear energy is a safe and clean source of power. Also, it provides a stable electricity production that is less demanding to infrastructure, unlike the intermittent delivery from solar and wind power which requires large investments in electricity grids to be able to cope with these variations. This is why many countries, both developed and developing, have adopted nuclear power to meet at least a part of their electricity needs.

Sweden has been utilizing nuclear energy since the 1970s, with 31% of its electricity being generated by six nuclear power plants in 2021 (SCB.se). Sweden once had a CO_2 neutral electricity production from about 1975 up until the year 1999, when the first NPP were shut down, because of political reasons. In 2023 this situation has become far worse with outright electricity deficits in the country, especially in the southern part of Sweden.

However, when examining nuclear energy, it is crucial to prioritize the main concern about its past, present and future use, which is the issue of radioactive waste. Around 12,000 tons of spent nuclear fuel is predicted to generate from the currently running Swedish nuclear facilities[1], [2] up to year 2045. These wastes are extremely hazardous and require disposal in a location that is inaccessible to humans and the environment for hundred thousand of years, until their radioactivity levels match those of natural ores [2].

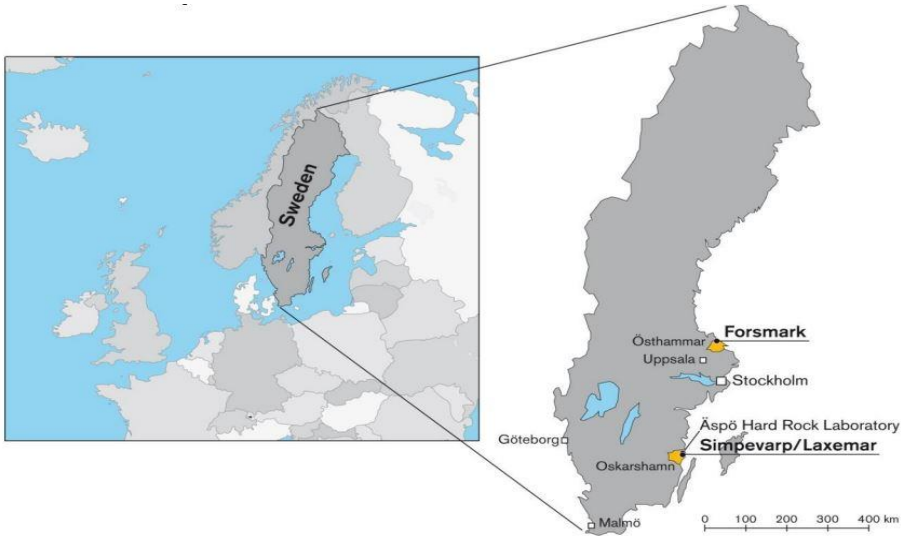

Figure 1-1: *Map of Sweden with the two locations of the SKB extended site characterisation areas in the municipalities of Östhammar (Forsmark) and Oskarshamn (Laxemar-Simpevarp)* [3].

To address this important issue, SKB, the Swedish Nuclear Fuel and Waste Management company, has conducted and financed research since 1970´s on the so-called KBS-3 concept for a final repository for spent nuclear fuel. The proposed final repository for managing the Swedish nuclear waste will be located in the Forsmark site in the municipality of Östhammar as shown in Fig. 1-1. The repository is designed to contain the spent nuclear fuel for up to 100 000 years [2].

This method, or rather concept, comprises the spent fuel encapsulated in corrosion resistant copper canister [4–6]. The canister is surrounded with a bentonite clay of low water permeability to prevent its direct contact with the ground water. The canisters will be disposed of at 400-500 meters depth in a seismic low activity zone of granitic rock formation as shown in Fig. 1-2.

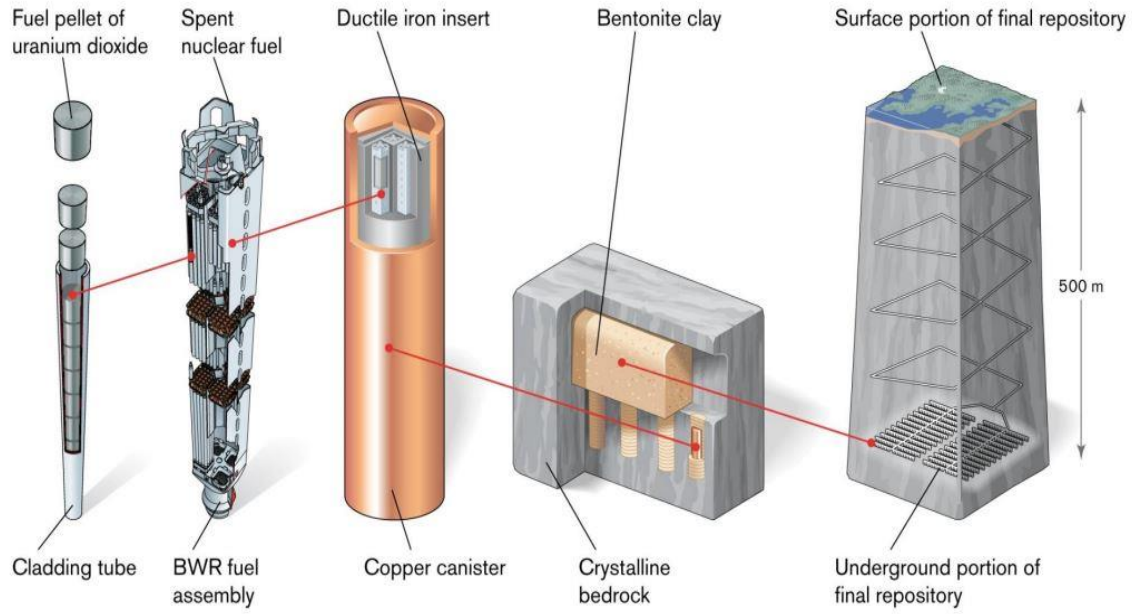

Figure 1-2: *The KBS-3 method for disposal of spent nuclear fuel* [7] (Copyright: Svensk Kärnbränslehantering AB).

In the event that the copper canisters fail, groundwater will come into contact with the waste and then the radioactive substances of the fuel may start to dissolve and be carried away with the groundwater. First the bentonite clay and then the granite rock are the layers that will initially come into direct contact with dissolved and the mobile radionuclide. In granite, there are essentially three zones that come into contact with radionuclides: 1) the fracture filling material 2) the disturbed zone of the rock matrix and finally 3) the undisturbed rock matrix. Despite very low porosity in the undisturbed granite matrix, there is still a significant retention capacity for radionuclides, especially if groundwater advection in fractures is very slow or nearly stagnant which may be the case if fractures are few in number and small in extension.

The granitic bedrock at the Forsmark site is characterized as having very few fractures and consequently this rock has, for typical Swedish bedrock conditions, a comparatively low hydraulic conductivity.

The particular rock in Forsmark is a granodiorite, composed primarily of feldspars, specifically plagioclase and K-feldspar, with the addition of minor components like biotite and chlorite [8-10].

Extensive research has been conducted by both SKB and the corresponding Finnish company POSIVA on the sorption of radionuclides onto granitic rock. The findings are primarily presented in the form of distribution co-efficients, also known as R_d values which are used in modelling radionuclide transport scenarios [11], [12].

Even if R_d values are simple to integrate in radionuclide transport modelling codes, there is a drawback since R_d values are only valid for a given chemical condition. If groundwater composition changes, the R_d values must be modified. Often this is done by crude inter or extrapolation from different datasets.

A more robust approach is therefore to utilize Surface Complexation Modelling (SCM), which is based on a detailed description of surface reactions with corresponding reaction constants. Such models can then be coupled with geochemical speciation codes like PHREEQC [13] and the impact on R_d values of changing groundwater composition can be calculated.

Here, the problem is usually the scarcity of studies that utilize SCM to interpret sorption distribution co-efficient. Also, SCM is only possible for pure and well-defined solid phases, hence, sorption experiments with the pure mineral phases have to be made and the complex rock must be modelled as a combination of SCM datasets for pure minerals, for example by using the Component Additivity approach (CA) [14–17].

To support a system understanding approach to radionuclide sorption in bedrock and to provide modelling data, the Swedish Radiation Safety Authority (SSM) have instigated this research as part of what the authority considered as one of the neglected topics in the research conducted by SKB about safety issues related to the final repository.

In this work the goal is to generate an appropriate large dataset of Rd values for one single mineral, so SCM can be made for the interpretation of the sorption data.

This work can therefore be seen as a first step in obtaining SCM parameters for granitic minerals to be used in a future modelling of sorption for the complex granite material. According to the literature, especially biotite, one of the granitic minerals, has a considerable capacity for sorbing dissolved radioactive cationic elements, [18–20]

When it comes to biotite, various studies have explored the radionuclide sorption on this mineral. However, only a few of them have utilized SCM to interpret the results. This is also true for the role of biotite in the sorption capacity of Forsmark granite[21].

Since SCM involves the assignment of specific reactions on a surface, the solid phase must be well-defined and characterized. Moreover, to make a robust SCM on experimental sorption data, a fairly large range of different experimental conditions must be investigated [22].

The aim of this investigation is therefore to carry out batch sorption experiments with a well-characterized biotite with four different elements (Cs (I), Ba (II), Co (II), and Eu(III)), five different pH values (5 to 9) and three different (0.001, 0.01 and 0.1 M) ionic strengths at 25ºC. The results is to be modeled using a combination of surface complexation and ion-exchange reactions, with specific reactions defined and equilibrium constants optimized through a combination of PHREEQC [13] speciation calculations and a PYTHON code optimization routine.

2. Background

To put this work into a context, a brief description of the main mineralogical features of the Forsmark site is given in this Section. This is followed by a description of the particular mineral that was chosen for this study, namely biotite, and a description of the methodology for modelling the sorption, the Surface Complexation Model.

A brief motivation for the choice of radionuclides is given next. This section concludes with a condensed version of Paper I, the literature review for previous SCM studies used in connection with biotite.

2.1. Some characteristics of the granitic bedrock

The proposed repository's targeted rock domain (identified by SKB code RFM029) mainly consists of a metamorphic medium-grained metagranite to granodiorite rock (SKB rock type code 101057), which falls under major group B, covering around 84% of the targeted rock domain RFM029. Other rock types present in the domain include fine- to medium-grained granodiorite, granite, and tonalite (10%), amphibolite (3%), and a small amount of pegmatite (2%) [23] .

Based on the thin section point-counting analysis of six samples, the mineralogical composition of this metamorphic medium-grained metagranite to granodiorite consists of different minerals as shown in Table 2-1.

Table 2-1

Mineral	**Formula**	**Percentage**
Quartz*	SiO_2***	26-39%*
Biotite*	$(K_{1.1}Mg_{0.7}Mn_{0.1}Ti_{0.2}Fe(II)_{1.9}Fe(III)_{0.1})Fe_{0.1}Al_{1.3}Si_{2.6}O_{10}(OH)$**	3-12%*
K-feldspar*	$(K_{0.82}Na_{0.25}Fe_{0.01})(Al_{1.07}Si_{2.92})O_8$**	14-29%*
Plagioclase*	$(Na,Ca)[(Si,Al)AlSi_2]O_8$***	27-41%*
Chlorite*	$Mg_{2.02}Ti_{0.03}Fe(II)_{1.33}Fe(III)_{0.15})(Al_{1.94}Si_{2.06})O_{10}(OH)_8$**	0-0.4%*
Muscovite*	$KAl_2AlSi_3O_{10}(OH)_2$***	0-1%*
Epidote*	$Al_2Ca_2FeH_2O_{13}Si_3$***	0-1%*
Titanite*	$CaTi(SiO_4)O$***	0-1%*
Zircon*	$ZrSiO_4$***	0-0.2%*

*[9], **[52], ***mindat.org

Despite having a lower mineral abundance than other minerals, biotite has a high retention capacity for radionuclides [18–20]. Therefore, biotite mineral was chosen for study in this work.

2.2. Biotite structure and properties

Biotite is a mica mineral, categorized as a sheet silicate, that adheres to a structural arrangement of Tetrahedral-Octahedral (TOT) layers of Si and O plus an interlayer cation (C), usually K^+.

Since Si (IV) is partially replaced with Al III), there is a net negative charge of a TOT layer which is compensated with the binding of the interlayer K^+ ions.

The cation therefore functions like a glue that binds the TOT layers together with electrostatic attraction. The thickness of a single layer of TOT+C in biotite can range from 9.5 to 10Å, and the repetition of this pattern constitutes the biotite mineral, shown in Fig. 2-1.

Biotite possesses various sorption sites that facilitate the binding of radionuclides through chemical (covalent or ionic) or physical (electrostatic) bonding [19], [25].

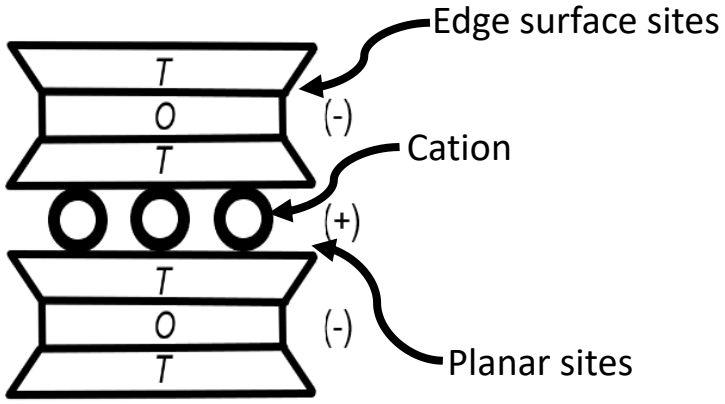

Figure 2-1: Schematic representation of the TOT+ C structure of biotite mineral

In a review on the solubility of sheet silicate minerals [26], it is suggested that the edge sites responsible for sorption properties of these minerals are mainly aluminol and silanol groups that can be protonated according to:

$$\equiv AlOH + H^+ \rightleftharpoons \equiv AlOH_2^+ \quad \text{(Eq.1)}$$

$$\equiv AlO^- + H^+ \rightleftharpoons \equiv AlOH \quad \text{(Eq.2)}$$

$$\equiv SiO^- + H^+ \rightleftharpoons \equiv SiOH \quad \text{(Eq.3)}$$

Binding to these sites is through the mechanism of **surface complexation**, that is through reaction that is similar to complex formation reactions in solution. The surface complex can be formed either with (outer sphere complex) or without (inner sphere complex) the hydration shell intact.

The most abundant surface sites, however, are the so called ditrigonal siloxane sites found on the basal plane of the tetrahedral sheet. These interlayer sites, or actually cavities, can bind cations by electrostatic attraction for neutralizing the inherent negative charge of the silicate structure of the mineral. The mechanism for binding the interlayer cations is an **ion exchange mechanism**, where one cation is replaced with another.

Although the binding to the ditrigonal sites is electrostatic, the binding of the cation can also be with or without its hydration shell intact, depending on how well the cation fits into the surface cavity [27]

In the literature review made for this work (Paper I), it was found that radionuclide sorption onto biotite is modelled with at least one type of surface complexation site, usually representing

sorption sites at the sheet edges and one type of ion exchange site for the basal planes. The edge sites are then usually modelled as either 1-pKa (acidic) or 2-pKa (amphoteric) sites.

However, other models with more type of sorption sites have also been used, often then they distinguish between “strong” and “weak” edge sites, where the strong sites are presumably surface complexation sites that binds with chemical bonds while weak sites bind cations with their hydration-shell intact, by electrostatic bonds. This can possibly translate to aluminol and silanol sites, respectively. Alternatively, there can be some additional ion exchange sites also on the edges, in literature these are usually called Frayed Edge Sites (FES).

To conclude, there are at least two mechanisms for sorption onto biotite: 1) surface complexation with the edge sites, which requires a specific charged surface site and 2) ion-exchange with basal plane cavities, where the negative surface charge comes from a positive charge deficiency in the silicate structure.

To confuse matters, both mechanisms can apparently bind through both inner-sphere (ionic or covalent bond without hydration shell) and outer-sphere (physical/electrostatic bond with hydration shell) type of binding.

A chemical bond, either covalent (electron sharing) or ionic (loose or gain of electron), can however, only exist if there is an inner sphere binding.

2.3. Surface Complexation modelling

Typically, the data on radionuclide sorption is collected as empirical R_d values (distribution coefficients) a conditional distribution coefficient that is applicable to specific conditions such as pH, ionic strength, temperature, etc. However, these values do not offer any insight into the underlying chemical reactions that are responsible for sorption. Another drawback is that they are only valid for exactly the same conditions that were used when they were determined. This makes R_d values to be less robust in modelling radionuclide transport when changing groundwater conditions are to be included in the model.

To gain a comprehensive understanding of these chemical reactions at solid surfaces, Thermodynamic Sorption Modelling (TSM), also called Surface Complexation Modelling (SCM) is applied. Hereafter, only the TSM designation is used.

This approach involves the assignment of detailed chemical reactions that are taking place at the interface of solid and liquid. The assigned reactions are based on certain measured mineral characteristics, knowledge of the surface groups present in the mineral and the type of model employed.

TSM is an important tool for comprehending how pollutants can be transported in groundwater and retained on geological media (i.e., rock, gravel, sand, and soils) in the environment. The pollutants can initially be airborne and transferred to the ground as fall-out or they can origin from the leaching of waste or mineral deposits. One example of natural pollutants are the toxic arsenic-containing minerals, where the contamination of drinking water is a problem [28]

Several studies, including those by Davis et. al. [29], Hayes et. al. [30] and Koopal et. al. [31], have extensively reviewed different TSMs like the Constant Capacitance Model (CCM), the Stern Model (also called the Diffuse Layer Model (DLM)), the Triple Layer Model (TLM), and the Charge-Distribution Multi-Site Complexation Model (CD_MUSIC). All these models consider electrostatic buildup effects on the surface. In contrast the Non-Electrostatic Model

(NEM) does not consider such effects. A brief explanation about some of these different models is given in Section 3.1 below.

2.4. The selection of radionuclides for the experiments

The spent fuel quantity and its properties are dependent on the nuclear power plants, NPP's, operational conditions and is characterized by burn-up, type of reactor, fuel composition, etc. Based on these reference scenarios for the Swedish nuclear power plants, SKB has evaluated the radionuclide inventory for the final spent fuel repository. There is a complete list of about 49 radionuclides found in spent nuclear fuel [32].

Of these radionuclides, there is a short-list of thirteen radionuclides (Table 2-2) based on 1) high radiotoxicity in combination with 2) long-term risks [33].

According to the Swedish safety case evaluation, this list comprises the highest-priority radiotoxic elements. Together with their long half-life and their potential for mobility to biosphere, the assessment of transport properties of these elements becomes one key criterion of safety assessment of the geological repository [19], [34], [35].

This list of radionuclides of special concern is also similar to what is chosen by SKB [32] for a Finnish nuclear repository safety calculation [36]. Since the actinoids in Table 2-2 are part of the four natural decay chains, the daughter radionuclides have also been taken into account for the radiotoxicity risk calculations.

Table 2-2: *The inventory of the thirteen most concerning radionuclides in the spent fuel matrix based on 1) high radiotoxicity in combination with 2) long-term risk due to slow decay* [33]

No.	Radionuclide	Comment
1.	Am-241	In Np decay chain
2.	C-14	Activation product
3.	Cl-36	Activation product
4.	Cs-137	Fission product
5.	I-129	Fission product
6.	Nb-94	Fission product
7.	Pu-238	In U decay chain
8.	Pu-239	In Ac decay chain
9.	Pu-240	In Th decay chain
10.	Pu-241	In Np decay chain
11.	Sr-90	Fission product
12.	U-234	In U decay chain
13.	U-238	In U decay chain

Among these nuclides ^{134}Cs, ^{133}Ba, ^{60}Co, and ^{152}Eu were chosen in this investigation as either primary (Cs) or analogous (Ba, Co, and Eu) radionuclides. As an alkaline earth metal Ba is analogue element to both Sr and Ra, all with s^2 outer electronic shells. The transition metal Co can be seen as analogue to Ni, with $[Ar]3d^7s^2$ and $[Ar]3d^8s^2$ electronic shells, respectively.

Ni is not on this list since it is not part of spent fuel but will be found as a neutron activation product of steel in long-lived intermediate-level waste and is therefore also of concern for long-

term radiotoxicity risks. The lanthanide Eu (III) is mainly an analogue element for the actinide Am(III) since they have similar electronic structures ([Xe]$4f^7s^2$ vs [Rn]$5f^7s^2$).

All four radionuclides are strong gamma emitters, essentially redox insensitive and exist as Cs(I), Ba (II), Co (II), and Eu (III) under the repository groundwater conditions [11], [37].

2.5. Literature study on TSM of selected radionuclide on biotite

2.5.1. Cs

For cesium it was found that the method of establishing a sorption isotherm is commonly used to study the behavior of Cs sorption onto biotite [38 - 42]. Although the impact of ionic strength was not investigated in these studies, one study [42] analyzed the effects of the primary electrolyte cation.

Based on these results, it appears that the concentration of Cs is a significant factor for sorption strength, which indicates that several sorption sites are filled up in sequence. Several references have used a [24], [40], [42], SCM model for the clay mineral illite [43], which utilizes three distinct cation-exchange reactions. Each site appears to dominate sorption within a specific concentration range for Cs. However, in one study a Langmuir isotherm was used [38], and in another a Freundlich isotherm [39] . The use of a Langmuir isotherm indicates that sorption of Cs can also be modelled as a surface complexation and not necessarily a cation exchange, although it may then be a “weak” (electrostatic bond) type of surface complex.

2.5.2. Ba

Also, for the alkaline earth metals, the sorption isotherm experiment is commonly used [24], [25], [38], [44], although a few studies have investigated also the influence of electrolyte ion strength [25] and the salinity of the simulated groundwater [24]. These studies have consistently found that the concentration of metal has an effect on sorption. Additionally, as the ionic strength or salinity increases, sorption decreases, most likely due to an increased competition for the available ion-exchange sorption sites.
Typically for alkaline earth metals, modelling was conducted using the very same three-site ion exchange model that is also used for Cs, which is based on the illite mineral [43]. However, [44] used the empirical Freundlich isotherm and [38] used a single site Langmuir isotherm to model their sorption data. Also, here any systematic studies with pH and ionic strength variations are missing.

2.5.3. Co

In one single study, [45] the sorption of a transition metal, Ni(II) onto biotite, was examined. In these studies, a constant tracer concentration was used while varying pH and electrolyte strength. The findings indicated that Ni absorption had a clear sorption "edge" at pH 7 and the impact of ionic strength on Ni sorption was minimal. To analyze the data, a model featuring a 1-pK_a surface complexation site (without surface charge inclusion) and one ion exchange site was utilized, which seems to be sufficient to describe Ni sorption in the investigated range of pH 3-9.5. On the other hand, the variation of ionic strength had little effect on Ni sorption. This reinforces the case for the surface complex. Any ion-exchange is less likely to take place.

2.5.4. Eu

Only two studies examined the sorption of a lanthanide onto biotite. Both used Eu (III) [45], [46] and both studies are of pH and ionic strength variation type with fixed tracer concentration

type and both studies identified a sharp sorption "edge" (the sorption increases steeply) around neutral pH, which is typical for an amphoteric/acidic surface site. One work [45] utilized a model with a 1-pK_a surface complexation site and one ion exchange site to fit the sorption data, seemingly using non-electrostatic model (NEM), excluding any possible effect of surface charge. In contrast, [46] employed only one ion-exchange site where a proton-exchange also must be presumed since sorption was found to be pH dependent.

3. Theory

In this section, an attempt has been made to provide a brief explanation about the theoretical background of the investigated system. This includes a brief overview of the sorption processes occurring on the mineral surface, available surface complexation models, the different types of experimental techniques implemented in order to characterize biotite and the batch sorption experiment.

3.1. Thermodynamic sorption models

There are various TSMs available, as mentioned earlier, their usage is typically dependent on three assumptions: 1) sorption takes place with a reaction with equilibrium constant and mass balances, 2) there are a fixed number of sorption sites available on a surface, and 3) an incorporation of electrostatic effects in sorption reactions by taking the electrostatic correction factor, also known as the coulombic effect, into account. The following is an overview of the models. However, in the case of a Non-Electrostatic Model (NEM), only 1) and 2) are considered.

3.1.1 Non-Electrostatic Model

Considering the reactions that can take place at the surface-solution interface there are usually three types [47].

1) inner sphere binding between surface site and a charged solution specie with a relatively short-range chemical or electrostatic bond between them,

2) outer sphere binding with a longer-range electrostatic bond between a surface group and a charged solution specie with the hydration shell intact, and

3) hydrophobic expulsion, this is the case when relatively hydrophobic ions are expelled from solution and accumulated at the surface.

In addition, all these reactions can be accompanied with an ion-exchange, especially in the case if the charge of the solid phase is a structural bulk property and not a property of a specific surface site. The basal planes of biotite are typical for this type of reaction.

Note that all these reactions can be assigned a reaction mechanism and reaction constants with mass balances. Only in the electrostatic models an additional non-specific interaction of ions attracted to a charged surface, the so-called diffuse layer, is also taken into account. Considering a surface reaction between dissolved component A and surface site ≡S it can be formally written as

$$\equiv S + A \rightleftharpoons \equiv SA \qquad \text{(Eq.4)}$$

The equilibrium constant, *K,* for this reaction can be written:

$$K = \frac{[\equiv SA]}{[A]\cdot[\equiv S]} \qquad \text{(Eq.5)}$$

Since there is a finite number of surface groups $[\equiv S]_{tot}$, the mass balance for *S* can be combined with Eq.5 to give the Langmuir isotherm:

$$K = \frac{[\equiv SA]}{[A]\cdot([\equiv S]_{tot-}[\equiv SA])} \quad \text{(Eq.6)}$$

The isotherm is described by the two constants K and the concentration of $[\equiv S]_{tot}$. This is one of the simplest forms of model for sorption. If it can be assumed that $[\equiv S]_{tot} >> [\equiv SA]$, which means conditions far from saturation then:

$$K \cdot [\equiv S]_{tot} = \frac{[\equiv SA]}{[A]} \equiv K_d \quad \text{(Eq.7)}$$

This is the linear sorption isotherm characterized by the distribution constant, K_d

However, from an experimental standpoint, what is usually measured, especially if A is a radioactive substance, is not a distribution of a single species but all the species at once, that is:

$$\frac{[A]_{sorbed}}{[A]_{aq}} = \frac{[\equiv SA]+[\equiv SAX]+[\equiv SAY]+\cdots.}{[A]+[AX]+[AY]+\cdots..} \equiv R_d \quad \text{(Eq.8)}$$

This measurable quantity is called the distribution coefficient R_d and, in the literature, it is often confused with the distribution constant K_d. However, K_d values are seldom measurable but must be modelled by fitting to a dataset of experimental R_d values. If there are multiple surface sites to consider (i.e. a multi-site Langmuir isotherm), the number of possible species of A in solution and on surface will of course be many more with further corresponding K_d to fit.

Since protons and hydroxide ions are also involved both in solution and surface reactions, R_d values are often measured as a function of pH. The ionic strength of a background electrolyte solution will also affect R_d values, so this parameter is also commonly varied. Variation of $[A]_{tot}$ is usually only of interest if saturation conditions of the sorption isotherm are to be investigated. This is a means to investigate the number of surface sites that are involved, since each sites are usually saturated at different $[A]_{tot}$, due to different site densities.

Since mineral surfaces usually involve silanol and aluminol groups which can be protonated or de-protonated according to Eq.'s 1-3, a strong dependency of R_d on the pH, especially for charged solution species, is usually what is found. This is evident in the so-called "sorption-edge" behavior, where the R_d values are rapidly increasing or decreasing within a narrow range of pH values.

Finally, the concentration of sorbed A, $[A]_{sorbed}$ in Eq.8 is, unlike A in solution $[A]_{aq}$, usually not measurable directly but have to be calculated from the mass balance from a reference value of added A to the system, that is $[A]_{tot}$, and the measured value of $[A]_{aq}$:

$$[A]_{sorbed} = [A]_{tot} - [A]_{aq} \quad \text{(Eq.9)}$$

To model sorption with NEM, a number of surface characteristics have to be determined separately: 1) the pKa values for acidic surface sites, this is usually done by titrations with electrode on solid phase suspensions, 2) the total acidic site density, here different methods can be used but the most common is the tritium exchange method (used in this work), 3) the cation exchange capacity (CEC), this can be measured with the NH_4-acetate method and 4) the specific surface area of the solid phase, which is usually measured with the BET method. The latter value is important to determine because surface species are usually normalized to the surface area of the solid and not its mass or volume.

In 1989, Hiemstra et. al. [48] introduced CD-MUSIC, a model that utilizes crystallographic or spectroscopic information to explain a mineral's surface chemistry, surface functional groups, acidity constants, and pHpzc (point of zero charge - the pH at which the surface charge is zero). A theoretical method to estimate surface site densities is to use Density Functional Theory (DFT) calculations.

3.1.2. Electrostatic Models

Electrostatic models are essentially extended versions of the NEM. These extended models also consider the negative effect of the charge of the surface on further sorption of ions with the same sign of charge. This charge may thus decrease sorption of ions to the surface and can be seen as an activity factor for surface sites/species.

In solution, the activity factor compensates for the charge interactions between bulk electrolyte ions and other dissolved charged species in non-ideal solutions, thereby reducing their effective concentration. This reduced effective concentration is called the activity. The standard state is usually an infinitely dilute solution with activity factors set to 1. For increasing ionic strength activity factors approach zero. Also, the more the charge is of a species, the lower the factor will be. Thus, activity is a more general formulation of the concentration, which is only applicable to ideal (= dilute) solutions.

Activity factors y_i can be calculated with different models, one commonly used for intermediate electrolyte concentrations is the Davies model:

$$\log y_i = -0.5 \cdot (z_i)^2 \left(\frac{\sqrt{I}}{1+\sqrt{I}} - 0.3 \cdot I\right) \quad \text{(Eq.10)}$$

Here z_i is the charge of ion i and I is the ionic strength of the solution.

According to the Gouy-Chapman hypothesis about a solid-solution interface [31], [49], the surface is perceived as a flat plane that can be charged by surface groups with a layer of ions carrying an opposite charge in the solution next to it. The concentration of these ions decreases as the distance increases. This layer is referred to as a diffuse double layer and the model is known as the Gouy-Chapman diffuse layer model (DLM). According to this theory the surface charge density σ (C/m^2) is related to the potential of the surface Ψ_0 by:

$$\sigma = (8RT\varepsilon\varepsilon_0 c \cdot 10^3)^{0.5} \cdot sinh\left(\frac{Z\Psi_0 F}{RT}\right) \quad \text{(Eq.11)}$$

Here ε is the relative dielectric constant of water, ε_0 is the permittivity of vacuum and c is the molar electrolyte concentration. Z is the ionic charge of electrolyte. Inserting the values of constants gives:

$$\sigma = 0.1174 c^{0.5} \cdot sinh(Z\Psi_0 \cdot 19.46) \quad \text{(Eq.12)}$$

The DLM assumes that ions in the solution can reach the inner surface and has no physical limits (they are point charges). This is unlikely to happen, so in an adjusted model, the Stern DLM, the ions have finite sizes and there is a limit for how many and how close ions can be relative to surface. This divides the region near the surface in two regions, one where ions form a monolayer on the surface and one region outside this, where the diffuse layer begins.

This model requires that at the interface between the two layers potential and charge density should balance each other:

$$\Psi_0 = \Psi_D \quad \text{(Eq.13)}$$

$$\sigma = -\sigma_D \quad \text{(Eq.14)}$$

More elaborate models exist like the Triple Layer Model (TLM), which distinguishes between inner and outer sphere bound ions. The TLM divides the surface into three layers: 0, β-(inner Helmholtz plane) and d – plane (outer Helmholtz plane). The 0-plane is the potential determining plane where the protonation and deprotonation occurs, while the β- (inner Helmholtz plane) is where ion-pair and outer sphere complex formation occurs. The diffuse layer is described by the d-plane.

To utilize the Stern-DLM theory for adjusting NEM for surface charge, one has to consider the interaction energy between surface and solution species in two parts:

$$\Delta G_{tot} = \Delta G_{chem} + \Delta G_{coul} \quad \text{(Eq.15)}$$

Since the total Gibbs energy $\Delta G_{tot} = -RT\ln K$ and the coulombic part is $\Delta G_{coul} = \Delta ZF\Psi_0$ one gets for a surface reaction

$$\equiv SA \overset{K}{\Leftrightarrow} \equiv S^- + A^+ \quad \text{(Eq.16)}$$

With equilibrium constant

$$K = \frac{\{S^-\}\cdot\{A^+\}}{(SA)} = K_{int} \cdot exp\left(\frac{-\Delta ZF\,\Psi_0}{RT}\right) \quad \text{(Eq.17)}$$

In Eq.17 K_{int} is defined as the intrinsic reaction constant while K is the apparent constant and is dependent on the surface charge via the surface potential Ψ_0. The latter can be calculated from Eq.12, provided that the surface charge density is known.

One may assign the exponential term in Eq.17 to be an activity coefficient for the charged surface specie S^- . This is more obvious if writing Eq. 17 as:

$$K = \frac{\{S^-\}\cdot\{A^+\}}{(SA)} = \frac{(S^-)\cdot\{A^+\}}{(SA)} \cdot exp\left(\frac{-\Delta ZF\,\Psi_0}{RT}\right) \quad \text{(Eq.18)}$$

The only obstacle that remains for the calculation of the activity factor for the charged surface specie is then to establish the charge density σ in Eq. 12. This can be done by utilizing a mass balance for charged surface species:

$$\sigma = F(\Sigma z_i \cdot (S^{z_i})_i) \quad \text{(Eq.19)}$$

Here F = 96490 C/mol and $(S^{zi})_i$ (mol/m^2) is the surface density (mol/m^2) of the individual charged surface species i with charge z_i.

Here one may realize that in order to calculate the charge density σ, one must first have assigned a NEM in order to have some start values for the surface densities of charged species.

Then, a set of initial activity factors are calculated, and the equilibrium constants can be modified with these to calculate a new set of surface densities, now adjusted with surface

charge effects. This procedure must be iteratively made until the surface densities S_i have converged to some final values.

However, if working with trace amounts, typically well below 10^{-6}M, the amount of sorbed species will be low and will not influence surface charge. Then it is possible to calculate the charge density from Eq.19 from the bulk amount of charged acidic sites, which is determined by their pK_a values, the pH value of solution and the electrolyte concentration.

In this study, the experimental distribution co-efficients, R_d, and titration data have been modelled using a 2-pKa non-electrostatic model.

This model was applied by coupling the geochemical speciation software PHREEQC version 3 [13] with the PYTHON code optimization programming routine through a program that have been made for coupling these two software packages together [50], [51].

4. Materials and Methods

4.1. Biotite: Sample origin and preparation

The biotite, which has the chemical composition $K_{1.1}(Mg_{0.7}Mn_{0.1}Ti_{0.2}Fe\ (II)_{1.9}Fe\ (III)_{0.1})\ Fe_{0.1}Al_{1.3}Si_{2.6}O_{10}(OH)$ is 99.90% pure [52] and was obtained with courtesy of Naturshistoriska Riksmuséet and was stated to origin from Risör, Norway. The similarity in geological conditions between Norway and Sweden makes the biotite suitable for this study. The biotite was prepared, and its specific surface area measured with the BET method that have been developed previously [52], [53].

According to this procedure, at first, the biotite was crushed by a knife grinding machine (IKA model M20) for 1 to 2 minute and then, the crushed biotite was sieved with 0.25 mm and 0.5 mm Retsch stainless steel sieves (Retsch) with the help of shaking machine (Retsch AS200**)**. The total sieving time was close to 1.5 hours, which was accomplished in two steps: 1) at high amplitude for 30 min. 2) At low amplitude for 1 hour. After sieving, the crushed biotite was washed with 90% ethanol until the clear ethanol appeared. The washed biotite was dried in a vacuum chamber (Vacucell, MMM Group) for one week at a pressure of <30 mmHg.

4.2. Specific surface area measurement

Prior to analysis the biotite sample was dried for 24 h at a pressure of about 10μm Hg at the drying station of a gas-adsorption instrument (Micromeritics ASAP2020). Adsorption of Kr gas was used to measure the SSA of sample, and its results were evaluated using the BET-isotherm [54] by using the instrument's software.

4.3. Cation exchange capacity measurement

The ammonium acetate method was used for determination of the cation exchange capacity (CEC) of biotite mineral [55]. The experiment was conducted in triplicate, where one gram of biotite was mixed with 30ml of 1M ammonium acetate (Sigma-Aldrich, 99.99%) solution inside the 50ml polypropylene centrifuge tube (Oak Ridge, Thermo Scientific). The sampling was done six times in the progressive increase time intervals: 1, 2, 4, 8, 16, 32 days. Prior to each sampling, the two phases were separated with centrifugation (Beckman Coulter, Avanti J26S XP) at 20,000 rpm for 30 min, and then filtered through a 0.45μm polypropylene filter. The leachate was diluted 10 times with 0.5M nitric acid (Merck, Suprapur) and analysed with an Inductively Coupled Plasma Optical Emission Spectroscopy (ICP-OES) measurements (Thermo, iCAP XP Pro). The mathematical expressions that are used in order to calculate the CEC are given in section 2.2 of manuscript 2.

4.4. Biotite conditioning

The external surface of biotite usually contains impurities such as Ca^{2+} and K^{+}, which can affect the accuracy of the sorption experiments that were to be made with Na^{+} as the main background electrolyte. As a result, a portion of crushed biotite to be used in sorption experiments was purified and converted into a sodium form with as many Na^{+} ions as possible at the exchange sites. In order to achieve that the conditioning experiment was carried out. Three different solutions of sodium perchlorate, $NaClO_4$, (Merck, 98%) of 0.1M, 0.01M and 0.001M ionic

strength were prepared (pH = ~7) with ultrapure MilliQ water. The experiment was carried out in 10ml polypropylene tubes (Sarstedt). The solid and electrolyte were combined in the tube at a 1:50 ratio. The overall experiment length was at about 1.5 months to enable as much of Na exchange on the biotite as possible. The $NaClO_4$ solution was changed three times and their aliquots for the exchangeable cation were analyzed with ICP-OES (Thermo iCAP Pro XP Duo). The result shows that 80% of the biotite was converted for 0.01 M and 0.001M ionic strength and 31% in 0.1 M.

4.5. Biotite acidic site density measurement

The tritium exchange method of [56], [57] was used in order to estimate the acidic site density (ASD) of biotite. Following this method, a solution of 52MBq/mL tritium water (HTO) was made. 5g of crushed mineral was dispersed in 20 mL of 52MBq/mL HTO in a 50mL centrifuge tube (Oak Ridge 3119-0050, Thermo Scientific). A total of three tubes containing biotite were utilized, along with two tubes lacking any mineral as blanks. After a period of around three months of conditioning, the excess tritiated water was removed by centrifuging the tubes for 30 minutes at 20000 rpm. The opened tubes were then transferred to a hot plate in the fume hood to dry. Afterward, it was placed in a vacuum chamber (Vacucell, MMM Group) at a pressure of at <30mmHg and room temperature for 100 hours. In order to ensure sample dryness, the weight of the samples was checked periodically until the weight of the beaker/tube stopped changing. Afterwards, the dry mineral was transferred to a new tube and added only a minimal amount of slightly alkaline (pH 11) made ultrapure water. This new sample was initially placed under the ultrasonic bath (2 min.) and then on a shaking machine. This treatment was done to facilitate the extraction of bound radioactive protons. The sampling was done periodically up to ~57 days. Before each sampling the sample was first centrifuged for 30 minutes at 20000 rpm and then1mL of the supernatant was taken for LSC measurement. During the site density measurement, it was assumed that all radioactive protons bound to biotite had either been extracted or exchanged with non-radioactive protons. The amount N_H (mol/m^2) of extracted or exchanged acidic protons per surface area were calculated as:

$$N_H = \frac{A_t}{A_L S_{BET} M} moles\ m^{-2} \qquad \text{(Eq.20)}$$

Where A_t is the total specific activity of HTO in the new added water (cpm), A_L is the specific activity of HTO in the starting solution (cpm/mol HTO), S_{BET} is the BET surface area (m^2/g) and M represents the mass of biotite in gram.

4.6. Titration Experiment

To investigate the acid-base characteristics of the biotite mineral, the conventional continuous titration method was performed at room temperature. Standard solutions of 0.01M HCl and 0.1M NaOH (both Titrisol, Merck) were used for the titration. These solutions were made within the glovebox in an inert atmosphere.

An automatic titration instrument (905 Titrando, Metrohm) and a computer program (Tiamo v2.2, Metrohm) that controlled the amount and timing of addition were used to perform the titration. For pH monitoring, a glass electrode (Metrohm - 6.0250.010) was used. By monitoring signal stability after each addition, 15 min was selected as the fixed time difference between each addition. According to [15], [58], there are two main reasons why this was done.

First, it should be short enough to avoid dissolution of minerals, and second, it should be long enough to restore equilibrium to the system.

Prior to all the titrations, the electrode was calibrated with the Gran titration method [59]. The mineral titration was conducted in triplicate, utilizing 0.5 g of mineral that was dispersed in a 50 ml solution of 0.001M $NaClO_4$ electrolyte. In order to lower the initial pH level to ~3, 4 ml of 0.01M standard HCl was added. Following this, the suspension underwent titration using 0.1 M standard NaOH, with a fixed volume of 4 µl/addition. [15], [58].

4.7. Batch sorption experiment

In order to measure sorption R_d values of Cs(I), Ba(II), Co(II) and Eu(III) on a Na-converted biotite at different pH and ionic strengths, electrolytic solutions of 0.1M, 0.01M, and 0.001M $NaClO_4$ (Merck, 98%) were prepared. Each of these solutions were divided into five different solutions buffered to pH 5 with 1,4-Diethylpiperazine, 89% (DEPP, Alfa Aesar, 98%), pH 6 with 2-(N-Morpholino) ethanesulfonic acid (MES, Sigma-Aldrich, 99%), pH 7 with 3-(N-Morpholino) propanesulfonic acid (MOPS, Sigma-Aldrich, 99.5%), pH 8 with 1,4-Piperazinebis (propanesulfonic acid) (PIPPS, Merck, 98%), and pH 9 (DEPP). These buffers are recommended for their non-metal-complexation properties [60].

The buffer concentrations were 0.5mM for 0.001M and 5mM for 0.1M, 0.01M $NaClO_4$ solution respectively. These fifteen solutions were each spiked with radioactive Cs^+, Ba^{2+}, Co^{2+} and Eu^{3+}, all at about 10^{-8}M, in a mixture. The pH was then re-adjusted with 0.1M NaOH or 0.1M $HClO_4$.

The biotite was pre-conditioned in 0.001, 0.01 and 0.1M $NaClO_4$ solutions for 1 month and then centrifuged and electrolytes were removed.

The sorption experiment was conducted in triplicates at a temperature of 22-25°C. To prevent the formation of carbonato compounds and to minimize oxygen interaction, the experiment was carried out in a nitrogen-filled glovebox (MBraun InLab). 0.1g portions of Na-converted biotite with the particle size of 0.250-0.500 mm was put into the acid-washed 10ml polypropylene centrifuge tube (Oak Ridge 3119-0010, Thermo Scientific). These tubes were then transferred into the glovebox and 5mL of radioactive pH-buffered background electrolyte solution was added to give a solid-to-liquid ratio of 1:50. For the evaluation of wall sorption, separate blank samples were prepared without biotite. Additionally, acidic reference samples were also made for determining the concentration of reference radioactivity.

During the sorption experiment, samples were collected at specific intervals of 2, 14, 30, and 60 days. Prior to each sampling, the tubes were centrifuged (Avanti J26S XP, Beckman-Coulter) at 20000 rotations per minute for 30 minutes at a temperature of 18°C. An aliquot of 0.1ml (2%) from the supernatant was taken and mixed with 0.4ml 1M HCl buffer solution except the last sampling where straight 0.5ml was pipetted. The gamma activity of all four radionuclides in the aqueous phase was measured with an HPGe detector (GammaAnalyst with DSA2000 MCA and Genie2000 v.3.4.1 software, Canberra/Mirion).

R_d values were evaluated according to the mass balance formula [61]

$$R_d = \left(\frac{\bar{C}\cdot V_{ref}\cdot V_{out,n}}{A_{out,n}} - \left(V_0 - \sum_{i=1}^{n-1} V_{out,i}\right) - L_d - \frac{V_{out,n}\cdot\sum_{i=1}^{n-1} A_{out,1}}{A_{out,n}}\right)\cdot\frac{1}{m} \qquad \text{(Eq.21)}$$

$\bar{C}$ (cpm/L) is the average measured reference concentration, taken from the acidic references, V_{ref} (L) is the initially added volume of the radioactive solution, $V_{out,n}$ (L) and $A_{out,n}$ (cpm) are the volume and measured activity of sample *n* of the one to *n* consecutive samples. V_0(L) is the initial liquid volume of the batch, which includes V_{ref} and a residual amount of liquid from the preconditioning. L_d (L) is a factor compensating for wall sorption, measured in the separate blank series of batch experiments and m(g) finally, is the mass of the solid in the sorption experiment. The two summation terms in Eq.21stems from an overall mass balance and compensates for volumes and radioactivity that have been taken out in the consecutive samplings.

The wall sorption factor is calculated with essentially the same equation, however, since the mass participating in wall sorption is unknown, the wall sorption factor L_d (L) is defined as

$$R_{d,wall} \cdot m_{wall} = \left(\frac{\bar{C} \cdot V_{ref} \cdot V_{out,n}}{A_{out,n}} - \left(V_0 - \sum_{i=1}^{n-1} V_{out,i} \right) - \frac{V_{out,n} \cdot \sum_{i=1}^{n-1} A_{out,1}}{A_{out,n}} \right) \equiv L_d \qquad \text{(Eq.22)}$$

The pH of the batches was re-measured at the final sampling occasion, where small portions of the remaining liquid phase was taken out and measured. Also at last sampling, 1mL volumes of the remaining liquid were taken out and diluted to 5mL with 1M HCl (Suprapur, Merck) for biotite dissolution measurements using an ICP-MS (Thermo iCAP Q). For this, three standard series of 10, 50 and 200ppb Al, Si, Fe and Mg were prepared from 10ppm stock solutions (CPA Chem), utilizing 1M HCl and the three respective $NaClO_4$ electrolytes as blanks. 2 ppb Sc and In was added as internal standards to all samples and standard series.

5. Results and Discussion

The second manuscript contains a detailed explanation of all outcomes. Here, a brief synopsis of the obtained results is provided to highlight the information that can be obtained from this type of study.

5.1. Characterisation of biotite mineral

The Kr-BET analysis was used to determine the specific surface area (SSA) of crushed biotite. The calculated surface area for particle fraction 0.25-0.5 mm was found to be $0.4747 \pm 0.0021 \ m^2/g$. For comparison, the value for a Finnish biotite specimen reported by [42] gave $0.83 \ m^2/g$ for the same particle size fraction. This discrepancy can have numerous reasons. For example, it can be the use of different gases for surface area measurement. [38] The Kr-BET method used here is additionally 300 times more accurate than the N_2-BET method due to differences in the saturation pressures. Other explanations are natural variations in biotite and crushing and cleaning methods.

The CEC of the biotite mineral was determined by using the 1M ammonium acetate solution. The result suggests that the CEC of the biotite is $1.03 \pm 0.03 \, meq/100 \, g$. This measured value can be compared with literature values of 1.63 meq/100g [42] and $1.264 \pm 0.042 \ meq/100g$ [62] for other biotite specimen.

The applied tritium exchange method aims to evaluate the extent of exchanged tritium protons with protons that is accessible on mineral surface. This method has previously been used by [56], [57] to calculate the acidic site density of various mineral oxides. The experimental results, shown in Fig. 5-1, suggest that the acidic site density of biotite is $6.7 \pm 1.4 \times 10^{-6}$ mol/m^2 which is similar to the values reported in the literatures. However, these literature values were not experimental but obtained either by modelling in FITEQL computer software [41],[57] or by using the Density Functional Theory/molecular level modelling [63].

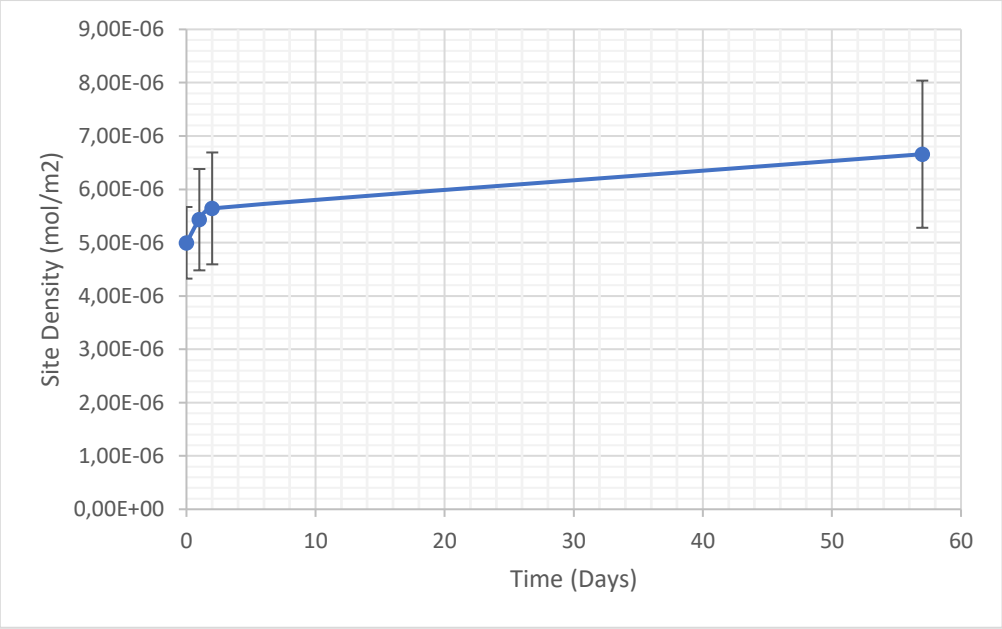

Figure 5-1: *Results for acidic site density measurements, using tritium exchange method*.

5.2. Titration Results

Fig. 5-2 shows the experimental (average of triplicates) and modelled titration results for 0.001M background electrolyte. The acquired titration data followed the typical s-pattern with one visible very minor hysteresis between pH 6 and 7, which was interpreted as the existence of at least one acidic site on the mineral surface. Following the suggested 2-pKa aluminol sites from literature[64], the acidity constants of this amphoteric surface hydroxyl group/sites were determined using PHREEQC software [50] coupled with a PYTHON code optimization routine assuming a two-site protolysis model with no electrostatic effect. The modelling outcomes in terms of acidity constants and site density are depicted in Table 5-1. The results are consistent with the findings of a previous investigation [65] pKa_1 = 4.6, pKa_2 = -6.4. A 1-pKa model was also tried but the fitting was worse than the 2-pKa model. For the best fit, the site density parameter was also fitted to the data, and this gave a value similar to the experimental value, using tritium exchange. Na sorption and cation exchange reactions were also used for fitting the titration data. Table 5-1 presents the constants for these reactions. However, the constant obtained from the cation exchange reaction (NaX) did not improve the fit for the sorption data. Hence, the batch sorption data was instead used to optimize this constant, resulting in a value of 3.63±0.40. The reason for the discrepancy is still unclear.

Table 5-1: *Optimized protonation ($\equiv SOH_2$) and deprotonation ($\equiv SO^-$), sodium inner ($\equiv SONa$) and outer ($\equiv SOHNa^+$) sphere complex and cation exchange (X) reactions for biotite in 0.001 M $NaClO_4$, along with corresponding reaction constants.*

Reactions	**Constants (log_K)**
$\equiv \mathrm{SOH} + \mathrm{H}^+ \rightleftharpoons \equiv \mathrm{SOH}_2$	4.77 ± 0.30
$\equiv \mathrm{SOH} \rightleftharpoons \equiv \mathrm{SO}^- + \mathrm{H}^+$	-6.82 ± 0.20
$\equiv \mathrm{SOH} + \mathrm{Na}^+ \rightleftharpoons \equiv \mathrm{SONa} + \mathrm{H}^+$	1.50 ± 0.09
$\equiv \mathrm{SOH} + \mathrm{Na}^+ \rightleftharpoons \equiv \mathrm{SOHNa}^+$	0.5 ± 0.05
$Na - X + H^+ \rightleftharpoons H - X + Na^+$	6.5 ± 0.10
Sorption site densities (mol)	
Acidic Site density	$8.13 \times 10^{-6} \pm 9.78 \times 10^{-7}$

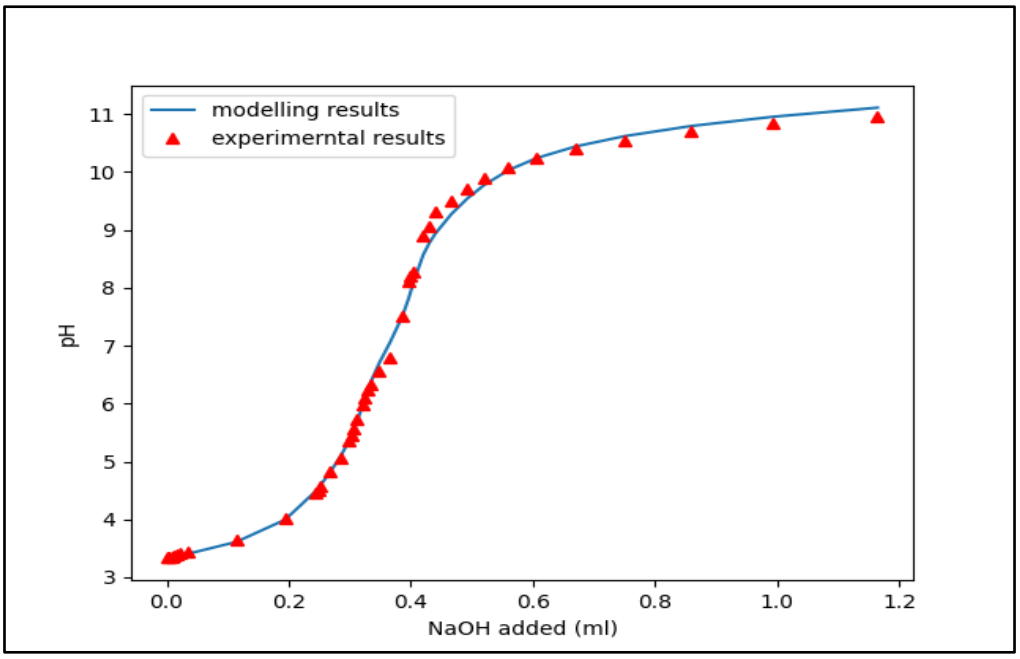

Figure 5-2: *Experimental (average of triplicates) and modelled titration curve for a suspension of biotite in 0.001 M $NaClO_4$.*

5.3. Sorption results

In this section the results of the main experiments, the radionuclide sorption studies, are presented.

5.3.1. Cesium sorption

Tables 5-2 to 5-4 show all the data collected for Cs sorption.

Table 5-2: *Sorption R_d (m^3/kg) results for Cs in 0.001 M $NaClO_4$.*

t (days)	Cs, pH 5	Cs, pH 6	Cs, pH 7	Cs, pH 8	Cs, pH 9
2	0.1	0.2	0.2	0.1	0.2
14	0.3	0.6	0.8	0.7	0.9
27	0.4	1.0	1.4	1.2	1.5
64	1.0	2.1	3.0	2.7	2.5

Table 5-3: *Sorption R_d (m^3/kg) results for Cs in 0.01 M $NaClO_4$.*

t(days)	Cs, pH 5	Cs, pH 6	Cs, pH 7	Cs, pH 8	Cs, pH 9
2	0.1	0.1	0.1	0.1	0.1
14	0.1	0.3	0.4	0.3	0.4
26	0.1	0.4	0.5	0.5	0.6
56	0.2	0.8	0.8	0.7	0.9

Table 5-4: *Sorption R_d (m^3/kg) results for Cs in 0.1 M $NaClO_4$.*

t(days)	Cs, pH 5	Cs, pH 6	Cs, pH 7	Cs, pH 8	Cs, pH 9
2	0.04	0.07	0.07	0.07	0.04
14	0.05	0.14	0.14	0.13	0.12
30	0.05	0.04	0.14	0.11	0.13
56	0.06	0.22	0.26	0.20	0.21

Fig. 5-3 shows the time-dependency of the 0.001 M experiments.

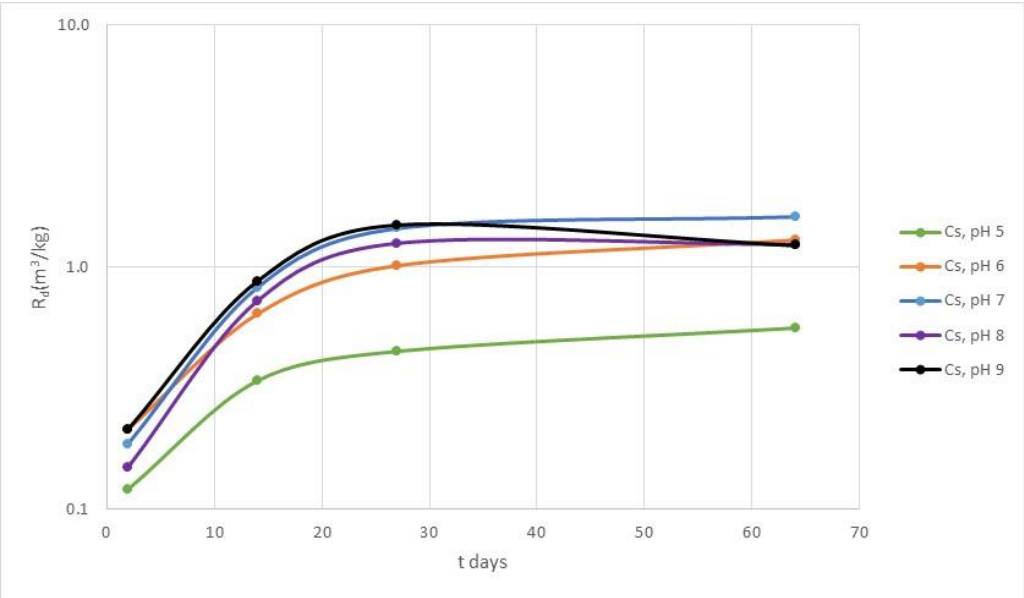

Figure 5-3: *Measured R_d values for Cs sorption onto biotite in 0.001M $NaClO_4$ versus time.*

Fig. 5-4 provides an illustration of the contribution of different Cs(I) sorption species in its sorption as an example and Fig. 5-5 depicts the findings of Cs(I) sorption as a function of pH at ionic strengths 0.0001, 0.01 and 0.1 M respectively, together with the results of model fitting. The outcome shows that:

- Equilibrium have been reached (Fig.5-3).
- Cs sorption by ion exchange is typically thought to be pH independent because an exchange with H^+ is considered negligible and exchange would instead be dominated by cations from background electrolyte like Na^+. However, this does not appear to be the case. A strong pH influence on Cs sorption is apparent for pH 5, with a considerably decreased Cs uptake compared with sorption at higher pH (Fig. 5-5).
- Typically for ion-exchange, the sorption of Cs decreases with the increase in ionic strength of background electrolytic solution (Fig. 5-5).
- Because Cs is affected by both pH and ionic strength. This suggests that Cs can sorb via both surface complexation and ion exchange.
- Higher ionic strength only suppresses the ion exchange reaction, the surface complexation reaction remains at about same R_d value.
- Cs sorption was modelled with a combination of ion exchange on the external basal surface and surface complexation on edge sites.

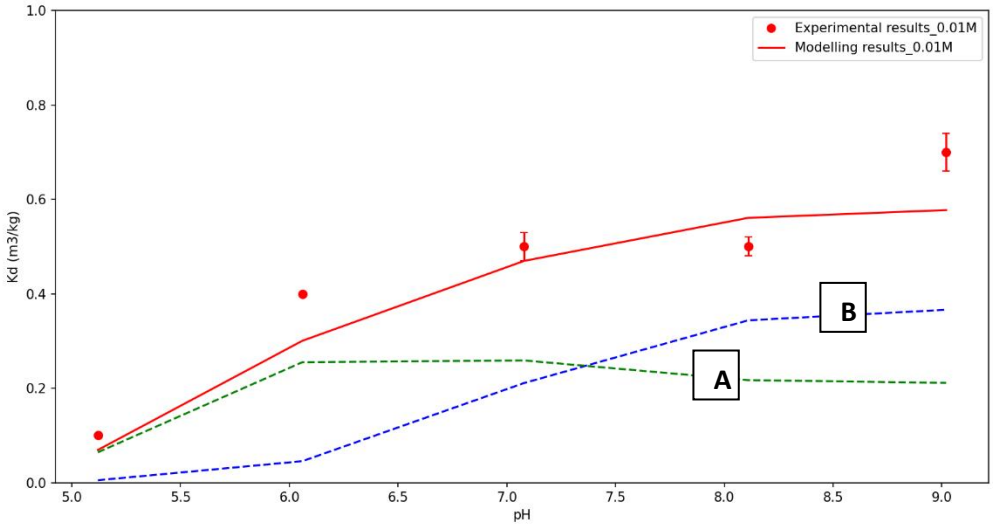

Figure 5-4: *An example figure for Cs sorption measurement (symbol) and modelling (continuous line) on biotite mineral in 0.01 M $NaClO_4$ solution. The contribution of different Cs(I) species in its sorption is represented by different curves: (A) CsX; (B) ≡SOCs*

The experimental data for Cs were modelled using only one surface complexation, ≡ SOCs, and one ion-exchange, CsX, site. The model appears to fit the data fairly well for all ionic strengths considering that a complete equilibrium may not have been reached. The implemented reactions together with the corresponding log K values are shown in Table 5-5 below:

Table 5-5

Reaction	**Log_k**
$\equiv \mathrm{SOH} + \mathrm{Cs}^+ \rightleftharpoons \equiv \mathrm{SOCs} + \mathrm{H}^+$	3.79
$\mathrm{Na} - \mathrm{X} + \mathrm{Cs}^+ \rightleftharpoons \mathrm{Cs} - \mathrm{X} + \mathrm{Na}^+$	1.61

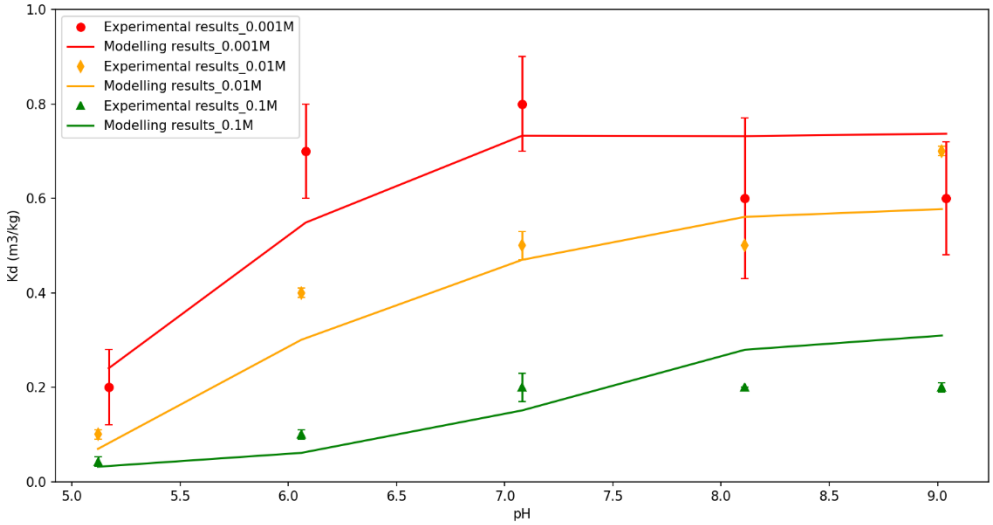

Figure 5-5: *Cs sorption measurement (symbol) and modelling (continuous line) on biotite mineral in 0.001 M, 0.01 M, and 0.1 M $NaClO_4$ solution.*

5.3.2. Barium sorption

Tables 5-6 to 5-8 show all the data collected for Ba sorption.

Table 5-6: *Sorption R_d (m^3/kg) results for Ba in 0.001 M $NaClO_4$.*

t(days)	Ba, pH 5	Ba, pH 6	Ba, pH 7	Ba, pH 8	Ba, pH 9
2	0.1	0.5	0.8	0.8	1.3
14	0.1	1.1	2.9	4.1	4.1
27	0.2	1.2	3.8	6.4	9.3
64	0.3	1.3	4.1	7.2	8.3

Table 5-7*: Sorption R_d (m^3/kg) results for Ba in 0.01 M $NaClO_4$.*

t(days)	Ba, pH 5	Ba, pH 6	Ba, pH 7	Ba, pH 8	Ba, pH 9
2	0.1	0.1	0.1	0.1	0.1
14	0.1	0.3	0.4	0.3	0.4
26	0.1	0.4	0.5	0.5	0.6
56	0.2	0.8	0.8	0.7	0.9

Table 5-8: *Sorption R_d (m^3/kg) results for Ba in 0.1 M $NaClO_4$.*

t(days)	Ba, pH 5	Ba, pH 6	Ba, pH 7	Ba, pH 8	Ba, pH 9
2	0.04	0.07	0.07	0.07	0.04
14	0.05	0.14	0.14	0.13	0.12
30	0.05	0.04	0.14	0.11	0.13
56	0.06	0.22	0.26	0.20	0.21

Fig. 5-6 shows the time-dependency of the 0.001 M experiments.

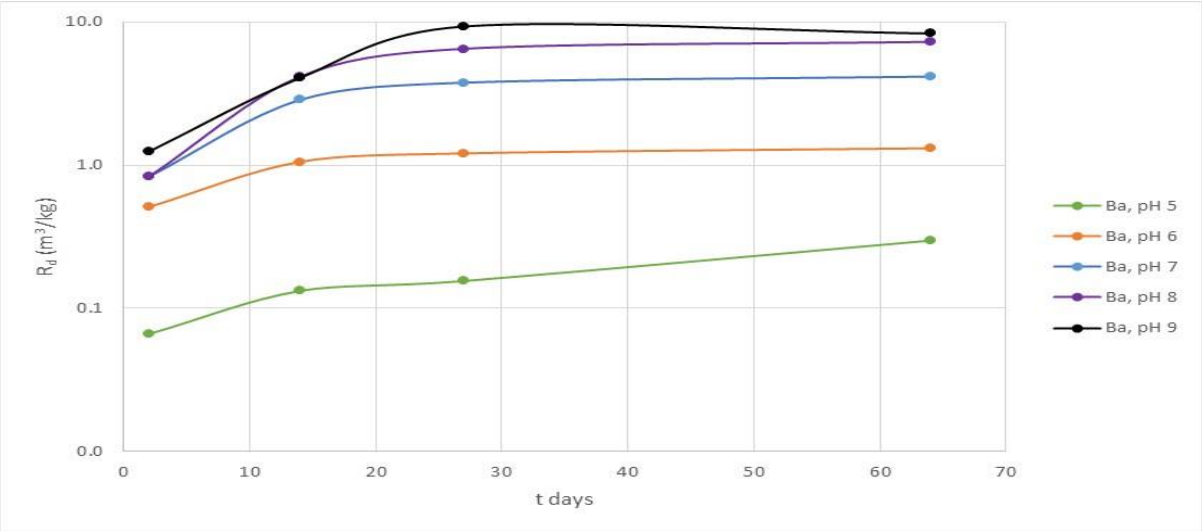

Figure 5-6: *Measured R_d values for Ba sorption onto biotite in 0.001 M $NaClO_4$ versus time.*

The experimental R_d values together with fitted models, for Barium (II) on biotite are shown in Fig. 5-8 for 0.001, 0.01, 0.1M ionic strengths respectively. The outcome shows that:

- Equilibrium have been reached (Fig. 5-6).
- The sorption of Ba(II) is both pH and ionic strength dependent (Fig. 5-8).
- Ba sorption is more due to surface complexation and less due to ion-exchange. This is also evident in the increased pH dependency of sorption, when compared with Cs (Figs. 5-3 and 5-6) with an increased spread of final R_d values.
- Ba sorption was modelled with a combination of ion exchange on the external basal surface and surface complexation on edge sites.

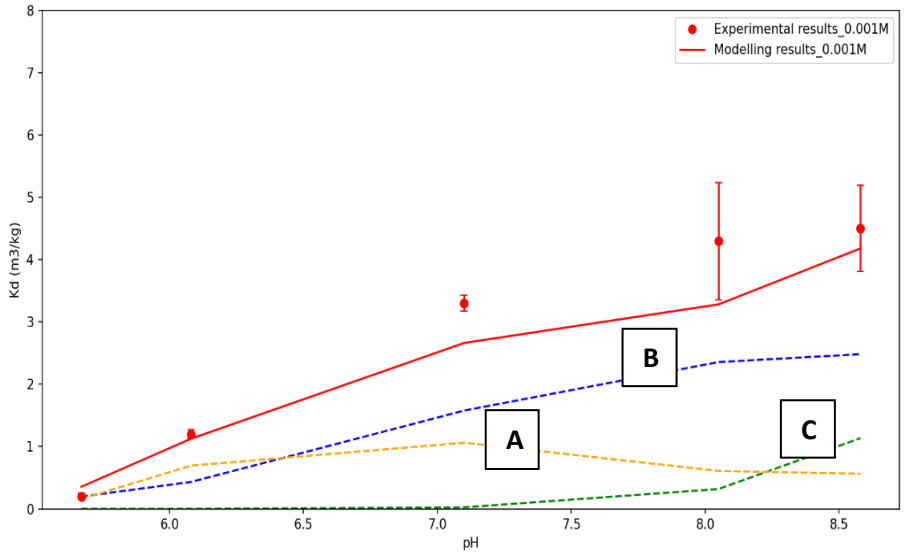

Figure 5-7: *An example figure for Ba sorption measurement (symbol) and modelling (continuous line) on biotite mineral in 0.001 M $NaClO_4$ solution. The contribution of different Ba(II) species in its sorption is represented by different curves:(A: Yellow line) BaX_2; (B: Blue line) $\equiv SOBa^+$; (C: Green line) $\equiv SOBaOH$.*

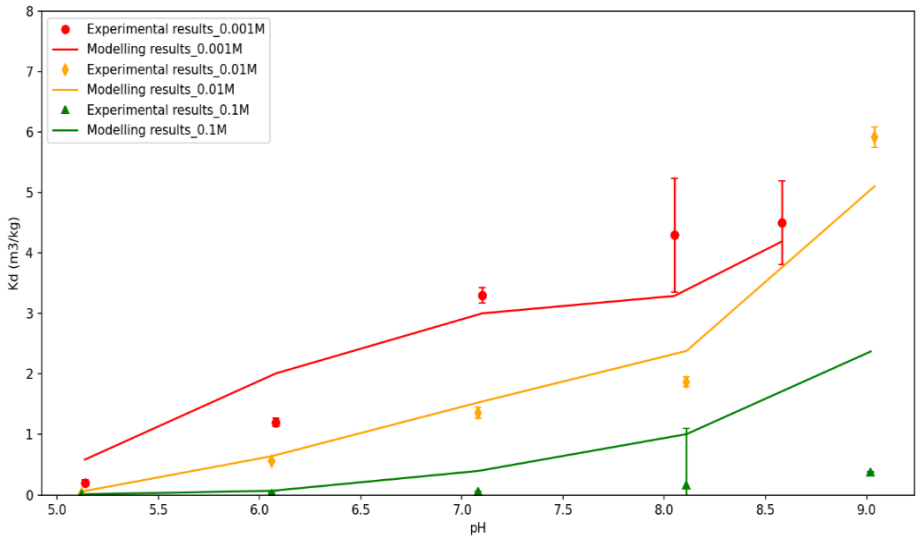

Figure 5-8: *Ba sorption measurement (symbol) and modelling (continuous line) on biotite mineral in 0.001 M, 0.01 M, and 0.1 M $NaClO_4$ solution.*

According to modelling results, two sites were found to be sufficient to reproduce the Ba (II) sorption data for each of the three background $NaClO_4$ concentrations (0.001 M, 0.01 M, and 0.1 M). The site includes two surface complexations, ≡ SOBa, ≡ SOBaOH, and one cation-exchange BaX_2 species as shown in an example Fig. 5-7. Table 5-9 below lists these species's reactions along with their respective constants.

Table 5-9

Reactions	**Log k**
$\equiv SOH + Ba^{2+} \rightleftharpoons \equiv SOBa^{+} + H^{+}$	-2.15
$\equiv SOH + Ba^{2+} + H_2O \rightleftharpoons \equiv SOBaOH + 2H^{+}$	-11.07
$Ba^{2+} + 2NaX \rightleftharpoons BaX_2 + 2Na^{+}$	0.40

5.3.3. Cobalt sorption

Tables 5-10 to 5-12 show all the data collected for Co sorption.

Table 5-10: *Sorption R_d (m^3/kg) results for Co in 0.001 M $NaClO_4$.*

t(days)	Co, pH 5	Co, pH 6	Co, pH 7	Co, pH 8	Co, pH 9
2	0.0	0.1	0.2	0.4	0.7
14	0.0	0.2	1.0	5.3	1.6
27	0.0	0.2	1.7	6.9	2.5
64	0.0	0.2	2.2	4.7	1.9

Table 5-11: *Sorption R_d (m^3/kg) results for Co in 0.01 M $NaClO_4$.*

t(days)	Co, pH 5	Co, pH 6	Co, pH 7	Co, pH 8	Co, pH 9
2	0.0	0.1	0.3	0.7	0.4
14	0.0	0.1	1.8	4.0	1.9
26	0.0	0.1	2.1	6.5	2.2
56	0.0	0.1	1.6	7.1	3.3

Table 5-12: *Sorption R_d (m^3/kg) results for Co in 0.1 M $NaClO_4$.*

t(days)	Co, pH 5	Co, pH 6	Co, pH 7	Co, pH 8	Co, pH 9
2	0.0	0.0	0.1	0.3	0.2
14	0.0	0.0	0.3	2.8	0.5
30	0.0	0.0	0.4	4.4	0.9
56	0.0	0.0	0.5	4.6	1.8

Fig. 5-9 shows the time-dependency of the 0.001 M experiments.

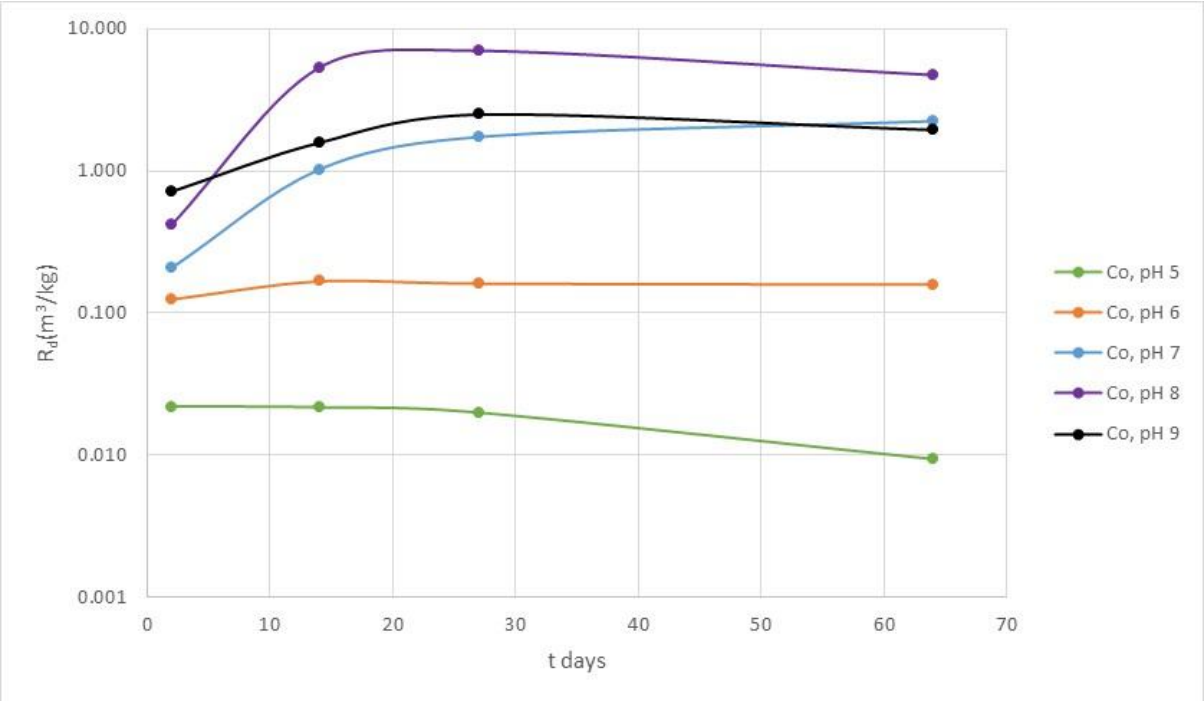

Figure 5-9: *Measured R_d values for Co sorption onto biotite in 0.001 M $NaClO_4$ versus time.*

Co (II) sorption results, including experimental data fitting, are presented in Fig. 5-11 for 0.001, 0.01 and 0.1 M $NaClO_4$, respectively. The main outcomes of the experiment are as follows:

- Equilibrium have been reached (Fig. 5-9).
- The sorption of Co is mainly pH dependent, ionic strength had little effect (Fig. 5-11).
- Co sorption was modelled with a combination of ion exchange on the external basal surface and surface complexation on edge sites.
- Co sorption is almost entirely due to surface complexation, the contribution from ion-exchange is negligible and was excluded from the model.
- This is also evident in the pH dependency of sorption, when compared with Cs (Fig. 5-3) and Ba (Fig.5-6) with a large spread of final R_d values (Fig. 5-9).
- The impact of Co hydrolysis is evident in the result for pH 9, where sorption is less than at pH 8. This can be due to its tendency to form strong hydroxide complexes.
- Co sorption is only weakly dependent on ionic strength (Fig. 5-11), which is in line with the view that surface complexation should be almost independent of ionic strength. since Na^+ complexation is weak.

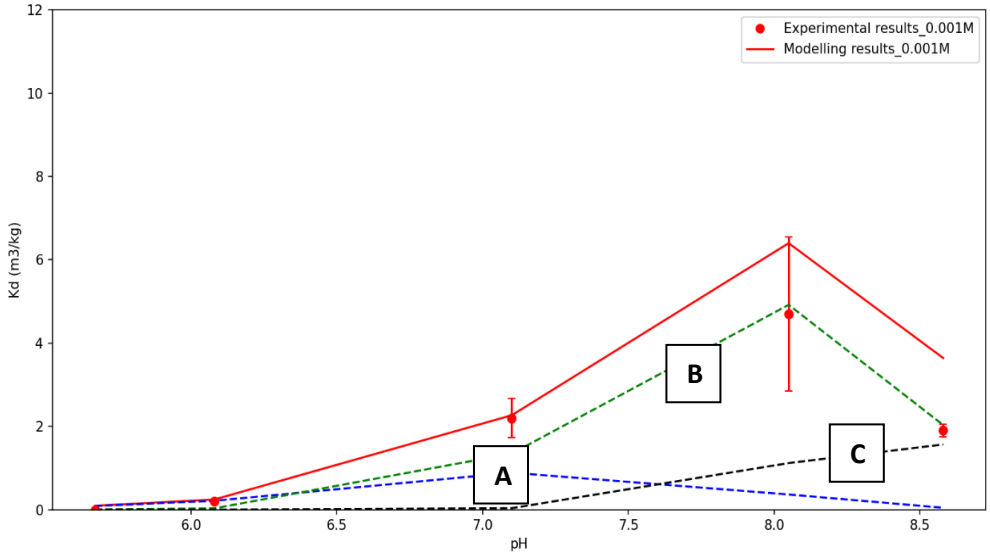

Figure 5-10: *An example figure for Co sorption measurement (symbol) and modelling (continuous line) on biotite mineral in 0.001 M $NaClO_4$ solution. The contribution of different Co(II) species in its sorption is represented by different curves: (A: Blue line)≡$SOCo^+$; (B: Green line)≡SOCoOH; (C: Black line) ≡ $SOCo(OH)_2^-$.*

The modeling of Co sorption data was done by taking only a surface complexation mechanism into account. The three surface complexation species ≡ $SOCo^+$, ≡ SOCoOH, and ≡ $SOCo(OH)_2^-$, Fig. 5-10, were used to describe Co sorption at all ionic strengths. The sorption reaction for the given species are shown in Table 5-13, below.

Table 5-13

Reactions	**Log_k**
$\equiv SOH + Co^{2+} \rightleftharpoons \equiv SOCo^+ + H^+$	-2.50
$\equiv SOH + Co^{2+} + H_2O \rightleftharpoons \equiv SOCoOH + 2H^+$	-9.42
$\equiv SOH + Co^{2+} + 2H_2O \rightleftharpoons \equiv SOCo(OH)_2^- + 3H^+$	-18.11

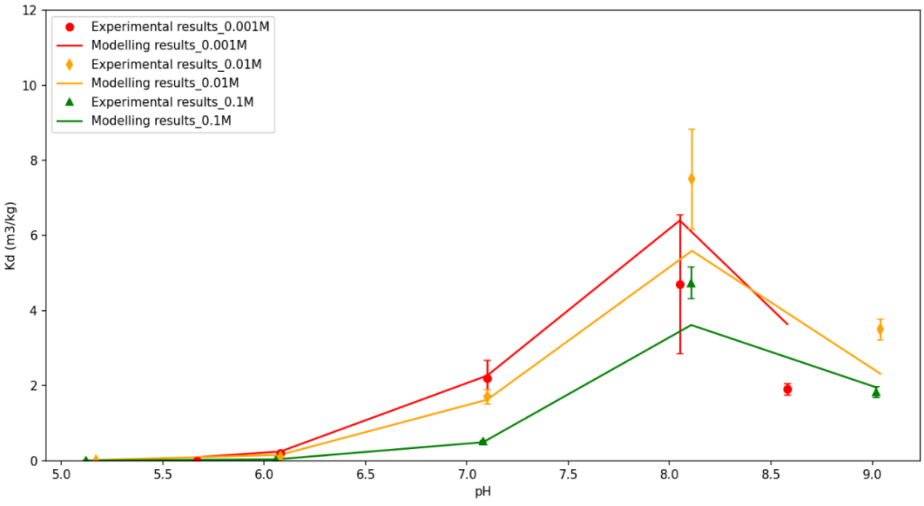

Figure 5-11: *Co sorption measurement (symbol) and modelling (continuous line) on biotite mineral in 0.001 M, 0.01 M, and 0.1 M $NaClO_4$ solution.*

5.3.4. Europium sorption

Tables 5-14 to 5-16 show all the data collected for Eu sorption.

Table 5-14: *Sorption R_d (m^3/kg) results for Eu in 0.001 M $NaClO_4$.*

t(days)	Eu, pH 5	Eu, pH 6	Eu, pH 7	Eu, pH 8	Eu, pH 9
2	0.5	1.9	1.4	0.7	0.8
14	3.4	7.0	4.1	2.4	1.8
27	3.4	7.9	5.0	4.7	3.0
64	4.5	18.3	8.5	5.1	2.7

Table 5-15*: Sorption R_d (m^3/kg) results for Eu in 0.01 M $NaClO_4$.*

t(days)	Eu, pH 5	Eu, pH 6	Eu, pH 7	Eu, pH 8	Eu, pH 9
2	0.1	7.3	10.0	2.5	0.4
14	0.2	10.0	15.0	7.8	1.8
26	0.1	20.5	20.0	9.0	1.6
56	0.1	2.9	4.2	4.0	1.7

Table 5-16: *Sorption R_d (m^3/kg) results for Eu in 0.1 M $NaClO_4$.*

t(days)	Eu, pH 5	Eu, pH 6	Eu, pH 7	Eu, pH 8	Eu, pH 9
2	0.6	1.3	2.2	1.8	2.1
14	2.4	5.4	10.7	15.0	2.7
30	1.1	10.0	20.0	25.0	1.0
56	2.0	6.0	6.7	2.2	3.0

Fig. 5-12 shows the time-dependency of the 0.001 M experiments.

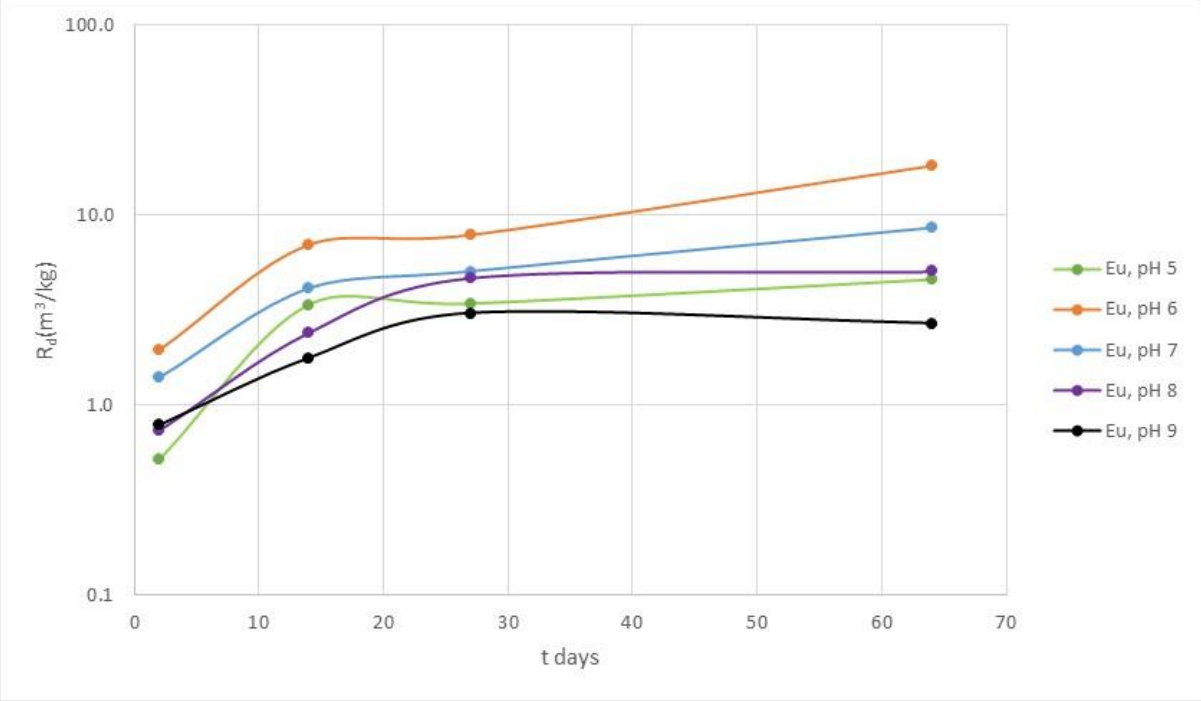

Figure 5-12: *Measured R_d values for Eu sorption onto biotite in 0.001M $NaClO_4$ versus time.*

Fig. 5-14 depicts the experimental and modeling results for Eu(III) sorption on biotite. The main outcomes of the experiment are as follows:

- Equilibrium has probably been reached (Fig. 5-12).
- The sorption of Eu is mainly pH dependent but shows some effects from ionic strength as well (Fig.5-14).
- Eu sorption was modelled with a combination of ion exchange on the external basal surface and surface complexation on edge sites.
- Eu sorption is due to a mix of surface complexation and ion-exchange.
- The pH dependency of sorption is larger when compared with Cs (Fig. 5-3), but smaller when compared with Ba (Fig. 5-6) and Co (Fig. 5-9), with the less spread in R_d values shown in Fig. 5-12.
- The lesser pH dependency for Eu sorption compared with Ba and Co is probably due to the very strong impact of Eu hydrolysis, where sorption maximizes at pH6 at 0.001M and is less at the higher pH values. This is due to competition from hydroxide that forms complexes of Eu.
- Contrary to Co, Eu sorption shows some dependency on ionic strength, which shifts the sorption maximum gradually from pH6 (0.001M) to pH7 (0.01M) to pH7.5 (0.1M). This is probably an effect of a gradually decreasing contribution of ion exchange at progressively higher ionic strength.

The modelling of Eu sorption on biotite for $NaClO_4$ solutions at concentrations of 0.001, 0.01, and 0.1 M was done by four surface species: $\equiv SOEu^{2+}$, $\equiv SOEu(OH)^{+}$, $\equiv SOEu(OH)_2$, and EuX3 as displayed in the example Fig. 5-13.

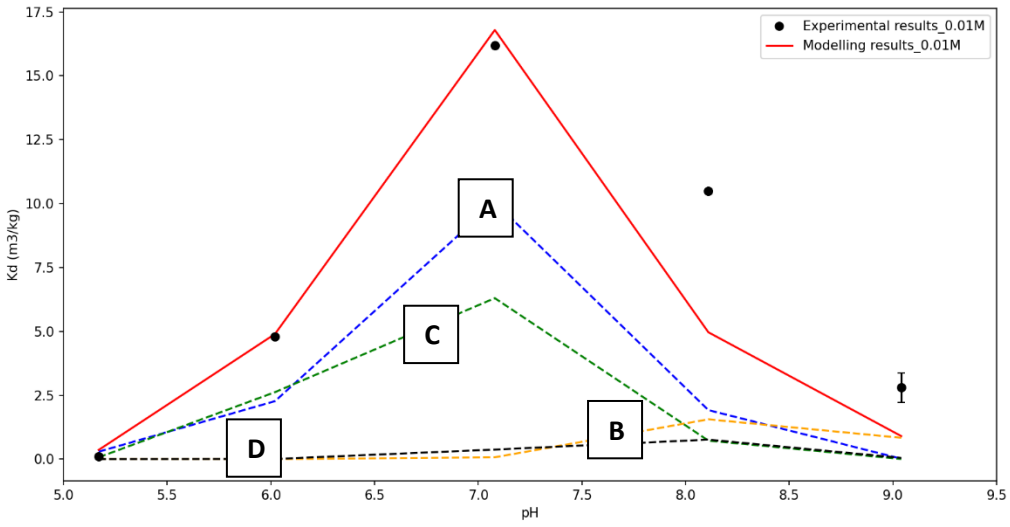

Figure 5-13: *An example figure for Eu sorption measurement (symbol) and modelling (continuous line) on biotite mineral in 0.01 M NaClO4 solution. The contribution of different Eu(III) species in its sorption is represented by different curves:* (A: blue line)≡ $SOEu^{2+}$*; (B: yellow line)*≡ $SOEu(OH)_2$*; (C: green line)* EuX_3*; (D: black line)*≡ $SOEu(OH)^{+}$

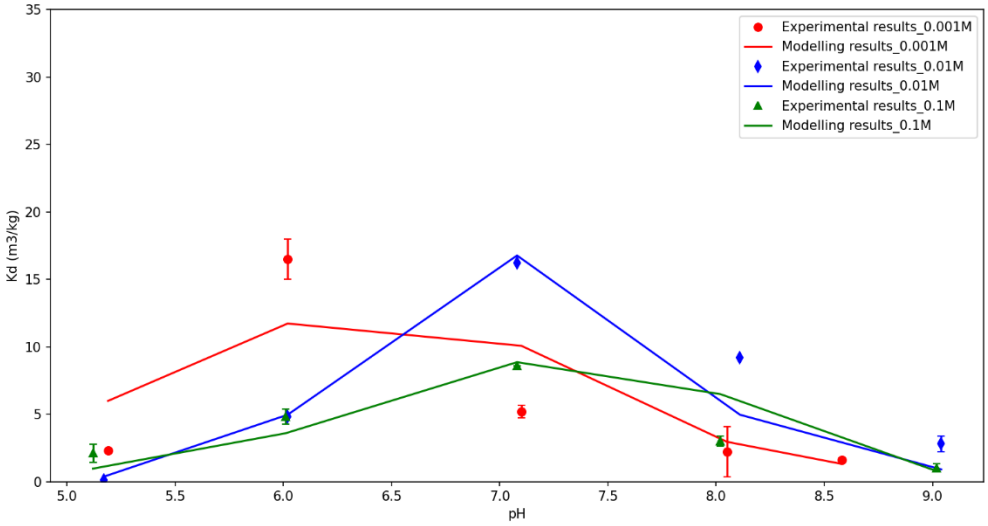

Figure 5-14: *Eu sorption measurement (symbol) and modelling (continuous line) on biotite mineral in 0.001 M, 0.01 M, and 0.1 M $NaClO_4$ solution.*

The reactions implemented in the model for surface complexation and ion exchange are provided in Table 5-17 below.

Table 5-17

Reactions	**Log_k**
$\equiv SOH + Eu^{3+} + H_2O \rightleftharpoons \equiv SOEu(OH)^{+} + 2H^{+}$	-9.5
$\equiv SOH + Eu^{3+} + 2H_2O \rightleftharpoons \equiv SOEu(OH)_2 + 3H^{+}$	-17.3

Reaction/Ionic Strength	**0.001M**	**0.01M**	**0.1M**
$\equiv SOH + Eu^{3+} \rightleftharpoons \equiv SOEu^{2+} + H^{+}$	Log_k = -1.80	Log_k = -0.99	Log_k = -0.46
$Eu^{3+} + 3NaX \rightleftharpoons EuX3 + 3Na^{+}$	Log_k = -2.53	Log_k = -0.21	Log_k = 2.65

6. Conclusions

In a separate tritium exchange experiment, the biotite acidic sites density was measured. The results are in line with previous studies. Additionally, the site density was optimized as a fitting parameter for the titration data gave, however, a slightly higher value.

The CEC and BET surface area values of the biotite specimens were consistent with earlier studies on other biotite samples.

On Na-converted biotite, the sorption of Cs, Ba, Co, and Eu was carried out over a two-month period at 25ºC under a variety of experimental conditions. All metals were found to be strongly influenced by the pH, for metals with weak hydrolysis (Cs and Ba) sorption increased with pH. For metals with strong hydrolyses, the sorption strength is maximized in the neutral pH range. Ionic strength also influenced sorption in those cases where ion-exchange participated, namely for Cs, Ba and Eu. For Co, on the other hand, its sorption was found to be almost independent of ionic strength.

The protolysis constants were determined through the modelling of titration results, which were then used to model the sorption experimental data. To simulate the uptake of all metals at trace concentrations, only one surface complexation site, known as ≡SOH, was considered. This site had a fixed acidic site density, and one planar cation exchange site with a fixed CEC was included. However, the electrostatic effect was not taken into account.

The sorption data fitting successfully yielded unique set of parameters for Cs, Ba, and Co. However, it seems difficult to obtain the same parameter for Eu species at all ionic strengths, aside from $\equiv \mathrm{SOEu(OH)^+}$ and $\equiv \mathrm{SOEu(OH)_2}$ surface complexes.

7. Future Work

The batch sorption experiment on biotite with Cs(I), Ba(II), Co(II), and Eu(III) at 40 and 60 ºC was also carried out in order to evaluate the impact of temperature differences on radionuclide sorption. The next step is to model the acquired sorption data and write the manuscript based on the gathered results.

The 2nd batch sorption experiment will be conducted similarly to the first, but with four different radionuclides (Ra, Am, Np and possibly with Th) at three different temperatures, three different ion strengths, five different pHs and three different temperatures 25, 40, and 60 ºC.

Then, using the available thermodynamic models and PHREEQC geochemical software combined with a PYTHON optimization routine, the sorption data from the second batch will be modelled. Based on the outcomes of the second batch, it planned to publish at least one manuscript.

8. Acknowledgements

The Swedish Radiation Safety Authority, SSM, is gratefully acknowledged for funding this project.

My most profound appreciation goes to my esteemed supervisors: Dr. Stellan Holgersson and Prof. Christian Ekberg for all your guidance, support, patience and always finding time for answering my questions even when you have lots of things to deal with.

In addition, I would like to thank Dr. Anna-Maria-Jakobsson for your invaluable feedback on my manuscript.

Friends, colleagues, lab mates, and the whole research team, thank you for your generosity, appreciation, motivation, encouragement, parties and being available for me in need.

Last but not least, I would like to thank my family for their endless support. It would be very hard to reach at this stage without your unconditional love, encouragement, and motivation.

9. References

[1] SKB, 'Long-term safety for the final repository for spent nuclear fuel at Forsmark Main report of the SR-Site project Volume III', Technical Report TR-11-01, 2011.

[2] SKB, 'Long-term safety for the final repository for spent nuclear fuel at Forsmark Main report of the SR-Site project Volume I', Technical Report TR-11-01, 2011.

[3] S. Berglund, U. Kautsky, T. Lindborg, and J. O. Selroos, 'Integration of hydrological and ecological modelling for the assessment of a nuclear waste repository', Hydrogeol J, vol. 17, 1, pp. 95–113, 2009, doi: 10.1007/S10040-008-0399-6.

[4] SKB, 'Nuclear Waste Containment Materials', Technical Report TR-01-25, 2001.

[5] L. Werme and S. N. Fuel, 'Design premises for canister for spent nuclear fuel Design premises for canister for spent nuclear fuel', Technical Report TR-98-08, SKB, 1998.

[6] P. Sellin and O. X. Leupin, 'The use of clay as an engineered barrier in radioactive-waste management - A review', Clays Clay Miner, vol. 61, 6, pp. 477–498, 2014, doi: 10.1346/CCMN.2013.0610601/METRICS.

[7] A. Hedin and P. Vidstrand, 'Safety Assessment Fundamentals Swedish Nuclear Fuel and Waste Management Company (SKB) Äspö Hard Rock Laboratory', 2019.

[8] L. Martin, 'Diffusive properties of granitic rock as measured by in-situ electrical methods', Royal Institute of Technology, Stockholm, 2004.

[9] E. Selnert, J. Byegård, H. Widestrand, and G. Ab, 'Forsmark site investigation Laboratory measurements within the site investigation programme for the transport properties of the rock', Technical Report P-07-139, 2008.

[10] M. Stenhouse, C. Jégou, P. Brown, G. Meinrath, H. Nitsche, and C. Ekberg, 'Review of SR-Can: Evaluation of SKB's handling of spent fuel performance, radionuclide chemistry and geosphere transport parameters External review contribution in support of SKI's and SSI's review of SR-Can', 2008.

[11] J. Crawford, 'Bedrock K d data and uncertainty assessment for application in SR-Site geosphere transport calculations', Technical Report R-10- 48, SKB, 2010.

[12] Posiva Oy, 'Safety case for the disposal of spent nuclear fuel at Olkiluoto. Models and data for the repository system 2012. Parts 1 and 2', vol. 31, pp. 828, 2013.

[13] D. L. Parkhurst and C. Appelo, 'Description of input and examples for PHREEQC version 3: a computer program for speciation, batch-reaction, one-dimensional transport, and inverse geochemical calculations', Techniques and Methods, 2013, doi: 10.3133/TM6A43.

[14] Å. Gustafsson, M. Molera, and I. Puigdomenech, "Study of Ni(II) sorption on chlorite - a fracture filling mineral in granites," MRS Online Proceedings Library 2004, vol. 824, 1, 316–321, 2004.

[15] A. M. Jakobsson, Y. Albinsson, and R. S. Rundberg, "Studies of surface complexation of H^+ , NpO_2^+, Co^{2+}, Th^{4+} onto TiO_2 and H^+, UO_2^{2+} onto alumina", Technical Report TR-98-15, SKB, 1998.

[16] D. A. Dzombak and F. M. M. Morel, 'Surface Complexation Modeling: Hydrous Ferric Oxide. A Wiley-Interscience publication', p. 393, 1990.

[17] J. Lützenkirchen, 'Surface complexation modelling', p. 638, 2006.

[18] M. S. Murali and J. N. Mathur, 'Sorption characteristics of Am(III), Sr(II) and Cs(I) on bentonite and granite', J Radioanal Nucl Chem, vol. 254, 1, pp. 129–136, 2002.

[19] R. M. Cornell, 'Adsorption of cesium on minerals: A review', J Radioanal Nucl Chem, vol. 171, 2, pp. 483–500, 2005, doi: 10.1007/BF02219872.

[20] O. Fabritius, E. Puhakka, X. Li, A. Nurminen, and M. Siitari-Kauppi, 'Radium sorption on biotite; surface complexation modeling study', Applied Geochemistry, vol. 140, 2022, doi: 10.1016/j.apgeochem.2022.105289.

[21] L. Sonnerfelt et al., 'Swedish Radiation Safety Authority SE-171 16 Stockholm Beredning av tillståndsansökan, SKB (slutförvar för använt kärnbränsle)', 2018.

[22] T. E. Payne et al., 'Guidelines for thermodynamic sorption modelling in the context of radioactive waste disposal', Environmental Modelling & Software, vol. 42, pp. 143–156, 2013, doi: 10.1016/J.ENVSOFT.2013.01.002.

[23] J. Byegård, E. Gustavsson, E.L. Tullborg, and J.O. Selroos, 'Bedrock transport properties, Preliminary site description Forsmark area -version 1.2', SKB Report R-05-86, 2006.

[24] E. Muuri et al., 'The sorption and diffusion of 133Ba in crushed and intact granitic rocks from the Olkiluoto and Grimsel in-situ test sites', Applied Geochemistry, vol. 89, pp. 138–149, 2018, doi: 10.1016/j.apgeochem.2017.12.004.

[25] M. Söderlund, H. Ervanne, E. Muuri, and J. Lehto, 'The sorption of alkaline earth metals on biotite', Geochem J, vol. 53, 4, pp. 223–234, 2019, doi: 10.2343/geochemj.2.0561.

[26] K. L, Nagy, 'Dissolution and precipitation kinetics of sheet silicates.' Reviews in Mineralogy and Geochemistry, vol. 31, 1, pp. 173-233, 1995.

[27] D. R. Ferreira, J. A. Thornhill, E. I. N. Roderick, and Y. Li, 'The Impact of pH and Ion Exchange on 133 Cs Adsorption on Vermiculite', J Environ Qual, vol. 47, 6, pp. 1365–1370, 2018, doi: 10.2134/JEQ2018.01.0043.

[28] S. Shankar, and S. Uma, 'Arsenic contamination of groundwater: a review of sources, prevalence, health risks, and strategies for mitigation.' The scientific world journal, 2014.

[29] J. A. Davis and D. Kent, 'Surface complexation modeling in aqueous geochemistry', Rev Mineral Geochem, 1990.

[30] K. F. Hayes, G. Redden, W. Ela, and J. O. Leckie, 'Surface complexation models: An evaluation of model parameter estimation using FITEQL and oxide mineral titration data', J Colloid Interface Sci, vol. 142, 2, pp. 448–469, 1991, doi: 10.1016/0021-9797(91)90075-J.

[31] L. K. Koopal, 'Chapter 3.5 Ion adsorption on mineral oxide surfaces', Stud Surf Sci Catal, vol. 99, pp. 757–796, 1996, doi: 10.1016/S0167-2991(06)81043-8.

[32] SKB, 'Radionuclide transport report for the safety assessment SR-Site', Technical Report TR-10-50, 2010.

[33] SKB, 'Spent nuclear fuel for disposal in the KBS-3 repository Spent nuclear fuel for disposal in the KBS-3 repository', Technical Report TR-10-13, 2010.

[34] M. Jaremalm, S. Köhler, and F. Lidman. "Precipitation of barite in the biosphere and its consequences for the mobility of Ra in Forsmark and Simpevarp.", Technical report TR-13-28, p. 203. Stockholm, Sweden: Swedish Nuclear Fuel and Waste Management, 2013.

[35] A. Hedin, 'Long-term safety for KBS-3 repositories at Forsmark and Laxemar-a first evaluation. Main Report of the SR-Can project.' 2006.

[36] Posiva Oy, 'Safety case for the disposal of spent nuclear fuel at Olkiluoto. Models and data for the repository system 2012. Parts 1 and 2', vol. 31, p. 828, 2013.

[37] J. Lehto, X. Hou, W.V. Wiley, and V. Gmbh, Chemistry and analysis of radionuclides: laboratory techniques and methodology, 2011.

[38] D. R. Brookshaw and J. R. Lloyd, 'Effects of Microbial Fe(III) Reduction on the Sorption of Cs and Sr on Biotite and Chlorite', vol. 33, 3–4, pp. 206–215, 2016, doi: 10.1080/01490451.2015.1076543.

[39] J. Lehto, E. Puukko, A. Lindberg, and M. Voutilainen, 'Batch sorption experiments of cesium and strontium on crushed rock and biotite for the estimation of distribution coefficients on intact crystalline rock', Heliyon, vol. 5, 8, 2019, doi: 10.1016/j.heliyon.2019.e02296.

[40] E. Muuri et al., 'Behavior of Cs in Grimsel granodiorite: sorption on main minerals and crushed rock', Radiochim Acta, 2016, doi: 10.1515/ract-2016-2574.

[41] E. Muuri et al., 'Cesium sorption and diffusion on crystalline rock: Olkiluoto case study', J Radioanal Nucl Chem, vol. 311, 1, pp. 439–446, 2017, doi: 10.1007/s10967-016-5087-8.

[42] J. Kyllönen, M. Hakanen, A. Lindberg, R. Harjula, M. Vehkamäki, and J. Lehto, 'Modeling of cesium sorption on biotite using cation exchange selectivity coefficients', Radiochim Acta, vol. 102, 10, pp. 919–929, 2014, doi: 10.1515/ract-2013-2180.

[43] M. H. Bradbury, B. Baeyens, 'A generalised sorption model for the concentration dependent uptake of caesium by argillaceous rocks', 2000.

[44] L. L. Ames, J. E. Mcgarrah, and B. A. W. Battelle, 'SORPTION OF URANIUM AND RADIUM BY BIOTITE, MUSCOVITE, AND PHLOGOPITE', 1983.

[45] E. Puukko, M. Olin, E. Puhakka, M Hakanen, and j Lehikoinen, 'Sorption of nickel and europium on biotite', In FUNMIG 3rd Annual Meeting, pp. 265–272, 2007.

[46] K. Fukushi et al., 'Sorption of Eu(III) on granite: EPMA, LA-ICP-MS, batch and modeling studies', Environ SciTechnol, vol. 47, 22, pp. 12811–12818, 2013.

[47] W. Stumm, J. Morgan, and J. Drever. "Aquatic chemistry." Journal of environmental quality 25, 5, 1996.

[48] T. Hiemstra, W. H. Van Riemsdijk, and G. H. Bolt, 'Multisite proton adsorption modeling at the solid/solution interface of (hydr)oxides: A new approach: I. Model description and evaluation of intrinsic reaction constants', J Colloid Interface Sci, vol. 133, 1, pp. 91–104, Nov. 1989, doi: 10.1016/0021-9797(89)90284-1.

[49] D. J. Shaw, 'Introduction to Colloid and Surface Chemistry', 1992.

[50] S. R. Charlton and D. L. Parkhurst, 'Modules based on the geochemical model PHREEQC for use in scripting and programming languages', Comput Geosci, vol. 37, 10, pp. 1653–1663, Oct. 2011, doi: 10.1016/J.CAGEO.2011.02.005.

[51] L. Wissmeier and D. A. Barry, 'Simulation tool for variably saturated flow with comprehensive geochemical reactions in two- and three-dimensional domains', Environmental Modelling & Software, vol. 26.2, pp. 210–218, 2011, doi: 10.1016/J.ENVSOFT.2010.07.005.

[52] I. E. Dubois, 'Specific surface area of some minerals commonly found in granite', Licentiate Thesis, Department of Industrial Ecology, KTH, 2011.

[53] I. E. Dubois, S. Holgersson, S. Allard, and M. E. Malmström, 'Dependency of BET surface area on particle size for some granitic minerals', Proceedings in Radiochemistry, vol. 1, 1, pp. 75–82, Sep. 2020, doi: 10.1524/RCPR.2011.0013.

[54] S. Brunauer, P. H. Emmett, and E. Teller, 'Adsorption of Gases in Multimolecular Layers', J Am Chem Soc, vol. 60, 2, pp. 309–319, 1938, doi: 10.1021/JA01269A023.

[55] C. J. Schollenberger and R. H. Simon, 'Determination of exchange capacity and exchangeable bases in soil—ammonium acetate method', Soil Sci, vol. 59, 1, pp. 13–24, 1945, doi: 10.1097/00010694-194501000-00004.

[56] Y. G. Bérubé, G. Y. Onoda, and P. L. de Bruyn, 'Proton adsorption at the ferric oxide/aqueous solution interface: II. Analysis of kinetic data', Surf Sci, vol. 7, 3, pp. 448–461, Jul. 1967, doi: 10.1016/0039-6028(67)90032-5.

[57] D. E. Yates, 'The structure of the oxide/aqueous electrolyte interface'. 1975.

[58] Å. Zazzi, A. M. Jakobsson, and S. Wold, 'Ni(II) sorption on natural chlorite', Applied Geochemistry, vol. 27, 6, pp. 1189–1193, 2012, doi: 10.1016/J.APGEOCHEM.2012.03.001.

[59] G. Gran, 'Determination of the Equivalence Point in Potentiometric Titrations. Part 11', 1952.

[60] Q. Yu, A. Kandegedara, Y. Xu, "Avoiding interferences from Good's buffers: a contiguous series of noncomplexing tertiary amine buffers covering the entire range of pH 3–11," Analytical Biochemistry, vol. 253, pp. 50-56, 1997.

[61] Andersson, M., H. Ervanne, M. A. Glaus, S. Holgersson, P. Karttunen, H. Laine, B. Lothenbach et al. 'Development of Methodology for Evaluation of Long-Term Safety Aspects of Organic Cement Paste Components. Posiva Working Report 2008-28. Posiva Oy, Olkiluoto, Finland.' (2008).

[62] X. Li et al., 'Multi-site surface complexation modelling of Se(IV) sorption on biotite', Chem Geol, vol. 533, 2020, doi: 10.1016/j.chemgeo.2019.119433.

[63] X. Li et al., 'Sorption of Se species on mineral surfaces, part I: Batch sorption and multi-site modelling', Applied Geochemistry, vol. 95, pp. 147–157, 2018, doi: 10.1016/j.apgeochem.2018.05.024.

[64] K.L. Nagy, 'Dissolution and precipitation kinetics of sheet silicates.' Reviews in Mineralogy and Geochemistry vol. 31, pp. 173-233, 1995.

[65] Y. Iida, T. Yamaguchi, T. Tanaka, and K. Hemmi, 'Sorption behavior of thorium onto granite and its constituent minerals', J Nucl Sci Technol, vol. 53, 10, pp. 1573–1584, 2016.